Elsevier Editorial System(tm) for Chemical Engineering Science
Manuscript Draft

Manuscript Number: CES-D-12-01773R2

Title: Extension and validation of the Particle Segregation Model for bubbling gas-fluidized beds of binary mixtures

Article Type: Regular Article

Keywords: Fluidization; Mixing; Multiphase flow; Particulate Processes; Drag force; Segregation.

Corresponding Author: Dr. Alberto Di Renzo, Ph.D.

Corresponding Author's Institution: University of Calabria

First Author: Alberto Di Renzo, Ph.D.

Order of Authors: Alberto Di Renzo, Ph.D.; Francesco P Di Maio; Vincenzino Vivacqua

Abstract: The present work elaborates on the Particle Segregation Model (PSM) recently developed (Di Maio, F.P., Di Renzo, A., Vivacqua, V., 2012. Powder Technology 226, 180-188) to address the prediction of the "segregation direction" in fluidized beds, i.e. the flotsam/jetsam behavior of the solid components in the bubbling bed. In the original derivation, the PSM was obtained in the limit of viscous flow, i.e. for particle Reynolds' number up to 5. In the present contribution we prove that its formulation is more general, and that it can be extended without modifications to any flow regime. Starting from the force balance on one particle, the competition of mechanisms in mixtures whose components' size difference effect counteracts that of density difference is contemplated. The macroscopic result is expressed, analytically and without adjustable parameters, in terms of the size ratio, density ratio, voidage and bed composition. The knowledge of the segregation direction can be combined with a comparison of the pure components' minimum fluidization velocities yielding, although only under the complete segregation hypothesis, a prediction of the different segregation/fluidization patterns. Extensive model validation is carried out by: (i) comparison of the predicted segregation direction against many experimental observations reported in the literature (53 systems) and with tests (7 systems) carried out in the present work; (ii) visualization in a 2D rig of segregated beds predicted to exhibit a layer fluidized below the stagnant rest of the material; (iii) observation of float/sink behavior of few large spheres immersed in the bubbling bed. Agreement for nearly all the considered systems is found, with remarkable segregation reversal predictions with bed composition for three of them.

UNIVERSITÀ DELLA CALABRIA
Dipartimento di Ingegneria per l'Ambiente e il Territorio e Ingegneria Chimica

Department of Environmental and Chemical Engineering
University of Calabria
Via P.Bucci, Cubo 44/A
87036, Rende (CS)
Italy

Manuscript Ref. : CES-D-12-01773

Dear Editor,

we would like to submit the revised version of the paper entitled "Extension and validation of the Particle Segregation Model for bubbling gas-fluidized beds of binary mixtures" by F.P. Di Maio, A. Di Renzo and V. Vivacqua, for consideration of publication in the journal *Chemical Engineering Science*.

The reviewer' comment has been considered by including additional text in the manuscript abstract. A reply to the Reviewer is attached with further details. Modifications applied to the revised abstract are highlighted in the attached "ManuscriptText_MarkedRevision" file. Finally, please note that our affiliation has changed since the submission and the updated name also appears among the marked changes.

The article contents is original and unpublished and is not being considered for publication elsewhere.

Yours sincerely,

On behalf of all authors,
Alberto Di Renzo

Corresponding author:

Dr. Alberto DI RENZO

Department of Environmental and Chemical Engineering
University of Calabria
Via P.Bucci, Cubo 44/A
87036, Rende (CS)
Italy

Tel: +39 0984 496654
Fax: +39 0984 496655
Email: alberto.direnzo@unical.it

Manuscript: CES-D-12-01773R1

Reply to the Reviewer' comments

Reviewer #1: Minor Revisions

R: *[…] Most replies to the reviewers questions/comments were answered or commented in a acceptable manner. However, in view of the reply given to question 4B of reviewer 1, the main purpose and application of Eq (24) must be specified in the abstract as these are hard to grasp.*

[Question 4B and our previous reply were:

R: *4 It is interesting to see a simple model equation (24), and happy to see it was validated by extensive experimental data. However, for this model equation there are several doubts:*

B) *Equation (24) contains the voidage <epsilon>, while it is not a known value for a fluidized bed, it is generally predicted by using continuity equations using multi-fluid model. Since the model presented in this paper contains such a generally un-known value it is hard to understand what is the general application scope for this equation. For what purpose can this model be useful?]*

A: The authors are not sure to catch the correct sense of the question. The particle segregation model is currently intended to apply at the global scale, where the voidage value is easily measurable during the experiments, knowing the charged mass of solids and bed height. Therefore, the applicability of the model in actual units is out of question. In numerical simulations the problem of the *local* voidage is solved by means of the equations and in order to apply the proposed model, arrangement of the formulation in terms of the local force balance on the different particle species would be necessary.]

A: Eq. (24) was presented with further details in our previous work (Di Maio et al., 2012), of which an extension is presented in the current manuscript. The Particle Segregation Model (PSM), Eq. (24) representing a key result, is a macroscopic tool to predict the segregation direction in complex fluidized mixtures as a whole. Therefore, it is a theoretical rather than computational model that could be useful in experimental or industrial applications.

The reviewer seems to refer to computational applications (like in e.g. multi-fluid models) of Eq. (24), which, as such, cannot find collocation. In other words, Eq. (24) is not expressible in differential terms. On the other hand, at the origin of Eq. (24) is a microscopic force balance applied to a single particle. Probably, it is this concept that could be possibly reused to derive other formulas applicable in computational (e.g. multi-fluid) models. However, presently such elaborations have little to do with the scope of the presented work (segregation problems in complex fluidized mixtures).

In the revised manuscript, additional text has been introduced in the abstract with the aim to help the reader focus on the correct, macroscopic nature of the PSM approach.

Graphical Abstract_HiRes.tif

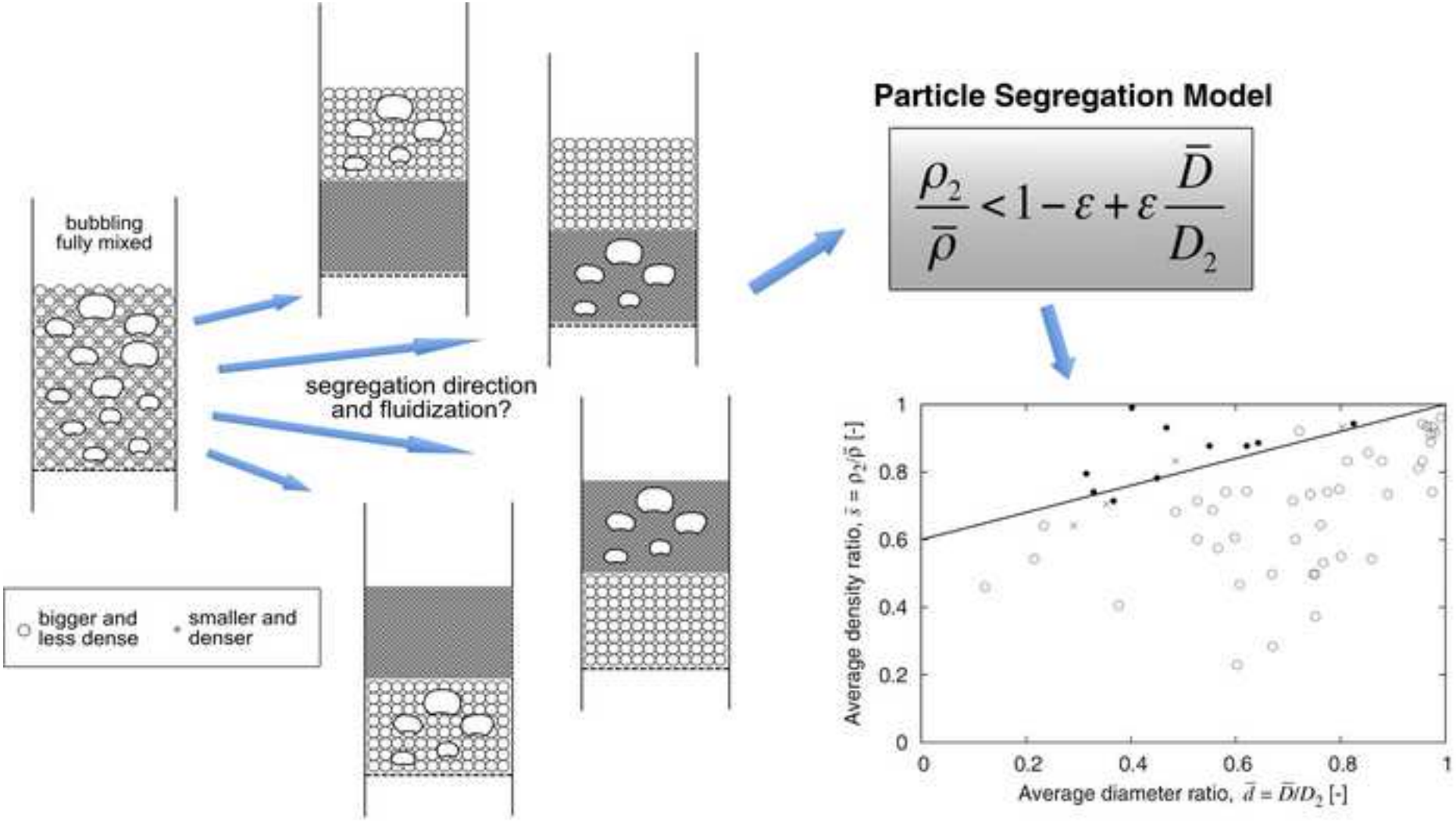

Highlights

- PSM predicts the segregation direction in a gas-fluidized binary mixture
- A general expression of the drag force for bi-disperse system is required
- The PSM formulation is proven for any flow regime without modifications
- Extensive comparison with flotsam/jetsam experiments shows agreement
- Cases with direction inversion with composition are studied experimentally

Extension and validation of the Particle Segregation Model for bubbling gas-fluidized beds of binary mixtures

Francesco P. Di Maio, Alberto Di Renzo*, Vincenzino Vivacqua

Department of Chemical and Environmental Engineering, University of Calabria
Via P. Bucci, Cubo 44A, 87036 Rende (CS), Italy

** Corresponding author (A. Di Renzo): T.: +39 0984 496654, F.: +39 0984 496655; Email: alberto.direnzo@unical.it*

Abstract

The present work elaborates on the Particle Segregation Model (PSM) recently developed (Di Maio, F.P., Di Renzo, A., Vivacqua, V., 2012. Powder Technology 226, 180–188) to address the prediction of the "segregation direction" in fluidized beds, i.e. the flotsam/jetsam behavior of the solid components in the bubbling bed. In the original derivation, the PSM was obtained in the limit of viscous flow, i.e. for particle Reynolds' number up to 5. In the present contribution we prove that its formulation is more general, and that it can be extended without modifications to any flow regime. Starting from the force balance on one particle, the competition of mechanisms in mixtures whose components' size difference effect counteracts that of density difference is contemplated. The macroscopic result is expressed, analytically and without adjustable parameters, in terms of the size ratio, density ratio, voidage and bed composition. The knowledge of the segregation direction can be combined with a comparison of the pure components' minimum fluidization velocities yielding, although only under the complete segregation hypothesis, a prediction of the different segregation/fluidization patterns. Extensive model validation is carried out by: (i) comparison of the predicted segregation direction against many experimental observations reported in the literature (53 systems) and with tests (7 systems) carried out in the present work; (ii) visualization in a 2D rig of segregated beds predicted to exhibit a layer fluidized *below* the stagnant rest of the material; (iii) observation of float/sink behavior of few large spheres immersed in the bubbling bed. Agreement for nearly all the considered systems is found, with remarkable segregation reversal predictions with bed composition for three of them.

Keywords: Fluidization; Mixing; Multiphase flow; Particulate Processes; Drag force; Segregation.

1. Introduction

Fluidized beds composed of more than one solid component are often encountered in industrial processing of granular materials. In many cases, the complex two-phase hydrodynamics of the bubbling regime leads to unpredictable segregation behavior that, in turns, severely affects the performance of key fluidization-based process units such as reactors, combustors, gasifiers, incinerators. As a consequence, their design is still dominated by empiricism. This is particularly true for charges involving irregular solids like most biomasses or municipal solid wastes (Cui and Grace, 2007). In other cases, the very aim of the unit is to drive the separation of two or more granular materials, like in mineral dressing and solids classification (Tanaka and Song, 1996; Olivieri et al., 2009).

In a bubbling gas fluidized bed, agitation due to bubbles is usually deemed responsible for the homogeneity of properties in the emulsion like temperature and gas-phase species concentration in the bed. However, if dissimilar solids are simultaneously utilized, their different fluidization behavior may lead to inhomogeneous solid composition along bed height, with the one component accumulated at the top usually referred to as *flotsam* and the other one as *jetsam* (Rowe et al., 1972). In some cases, segregation may prevail, typically at the lower velocities, with the suspended bed appearing as a superposition of two distinct bubbling layers. When the differences in properties are even more extreme, elutriation of one solid occurs before the full bed reaches suspension by the gas, rendering the fluidization of the whole mixture practically impossible. Generally, a gradually changing component distribution along bed height is observed.

Component properties in a fluidized mixture can also change as a result of the evolution of the chemical/physical process in the unit, leading to a progressive shift of a component location inside the bed and, possibly, local defluidization, with significant impact on the process performance (Ekinci et al., 1990).

Various papers in the literature report attempts at a characterization of the mixing and segregation patterns of binary mixture in bubbling gas-fluidized beds. Historically, significant progress in understanding multicomponent fluidization started in the seventies (Rowe et al., 1972; Rowe and Nienow, 1976; Nienow et al., 1978; Chiba et al., 1979). Numerous experimental works have since focused on the individual effect of size segregation and density segregation, or a combination of both (see e.g. Beeckmans and Stahl, 1987; Čársky et al., 1987; Hoffmann et al., 1993; Wu and Baeyens, 1998; Rasul et al., 1999; Rasul and Rudolph, 2000; Marzocchella et al., 2000; Formisani et al., 2001, 2008a; Gilbertson and Eames, 2001; Olivieri et al., 2004; Dahl and Hrenya, 2005;

Joseph et al., 2007; Jang et al., 2010). More recently, computational simulations have supplemented these investigations. Different research groups have utilized simulation approaches based on a two-fluid model (TFM) representation (Huilin et al., 2003; Gera et al., 2004; Qiaoqun et al., 2005; Owoyemi et al., 2007; Mazzei et al., 2010; Chao et al., 2012) or a combination of computational fluid dynamics and the discrete element method (DEM-CFD) (Hoomans et al., 2000; Bokkers et al., 2004; Feng et al., 2004; Feng and Yu, 2007; Di Renzo et al., 2008) to examine the phenomenon in more detail.

Attempts have been made at classifying and predicting the behaviors of binary mixture in gas-fluidized beds in terms of the particle properties and bed conditions. The first comprehensive 1-D differential model for segregation was proposed by Gibilaro and Rowe (1974). It is worth mentioning that later works showed that the evaluation of parameters in the general case is rather complicated (see e.g. Naimer et al., 1982). Among the studies devoted to the classification, the first simple and objective criterion to distinguish between the various categories was proposed by Chiba et al. (1980). Based on the analysis of the concentration profile of various solid pairs, they proposed conditions expressed in terms of combinations of size, density and minimum fluidization velocity of the two solids. An empirical criterion of mixability or non-mixability in fluidized beds was proposed by Tanaka et al. (1996), in which density and size ratios where combined with minimum fluidization voidage. Based on a relatively small amount of data, a line separating mixing and segregating beds was also proposed by Rasul et al. (1999). Recently, Rao et al. (2011) reviewed a significant number of data from the literature and carried out a few specific experiments to classify fluidized mixtures according to their observed behavior. All of these works are based primarily on the observations of real or simulated experiments, whilst a theoretical framework for a comprehensive understanding of the degree of mixing or segregation still lacks.

The full prediction of the concentration profile along bed height in the general case is a very complicated task. However, excluding trivial cases, even the question of which species in a segregating binary bed does play the role of flotsam, as opposed to jetsam, is essentially still open. It is well documented that a small size or density characterize solids that tend to float while larger or denser solids are typically found to sink to the bottom of the bed. When the two properties act in contrasting directions, the determination of the role of the two components (i.e. flotsam and jetsam) is far less trivial. It is convenient to start by considering an initially mixed bed and attempt to predict the possible segregation "direction" of the two species. Following the terminology introduced by Rowe and Nienow (1976), H and L will be used to denote higher and lower densities, respectively, and B and S to denote larger and smaller particle sizes, respectively. Thus, the focus

here will be on LB-HS mixtures. Traditionally, the difficulties arise because the mechanical equilibrium equations applied to the whole bed or to slices of the bed do not help, since in a fluidized bed the weight of every part of the system is balanced by the hydrodynamic action of the up-flowing fluid. Therefore, no information on the relative movement of the solids can be extracted and all segregation possibilities are admitted.

Additional complications arise when considering fluidization scenarios as they result from segregation patterns. Phenomenologically, segregation is stronger if higher velocities are avoided, as vigorous bubbling tends to favor bed mixing. On the other extreme, full bed suspension and particle mobility is a necessary requirement; otherwise, solids rheology may prevent the establishment of pure drag vs. gravity balance, additionally rendering the result dependent upon the initial pouring procedure. As a consequence, in focusing on the segregation tendency of a homogeneously mixed system, low velocities, slightly above the value required for bed suspension, should be most appropriate for our purposes. As particles' mobility allows segregation to take place, flotsam particles will be pushed upwards and jetsam particles will sink to the bottom of the bed. However, the flotsam is not necessarily the fluidized species, as there is no relation linking the tendency to segregate up or down *in the mixture* with the minimum fluidization velocity of the *pure* components. Therefore, four possible (simplified) segregation/fluidization scenarios can, in principle, be attained, as schematically depicted in Figure 1. In type A (Fig. 1a), the LB species is pushed to the surface (acting as flotsam), undergoing regular fluidization on top of the other component; in type B (Fig. 1b) the HS component segregates to the bottom of the bed, being fluidized as jetsam *below* the packed LB species; in type C (Fig. 1c) the HS component will float to the surface and get fluidized; in type D (Fig. 1d) the LB species will tend to act as jetsam and be fluidized below the packed bed of the other solid. However, not all cases are necessary plausible. Type A is certainly the most common condition observed, with the denser component packed at the bottom and the less dense species fully fluidized on top of it. Also, evidences of type-C segregation have been reported by Chiba et al. (1980). On the contrary, types B and D appear, at first, rather unexpected.

The present paper is aimed primarily at addressing the issue of the segregation direction in general and theoretically sound terms. The characterization of the segregation behavior of such systems will be proposed by working out a generalization of the Particle Segregation Model (PSM), as introduced by Di Maio et al. (2012). Previously, the model was restricted to low-Reynolds number flows, as it resulted from two conditions assumed: Carman-Kozeny relationship was utilized to express the drag force in monodisperse systems and van der Hoef et al. (2005) approach, derived in

the viscous-flow limit, was adopted to formulate the force in bi-disperse systems. It will be shown here that both origins of the limitation can be removed without amendments to the PSM formulation. In relation to the fluidization patterns developing as a result of the segregation (Fig. 1), an attempt will be made to model the observable fluidization/segregation scenarios as a function of the relevant system properties.

In Section 2 a derivation of the drag force for bi-disperse systems, required for the Particle Segregation Model, is presented in more general terms than previously (Di Maio et al., 2012). Section 3 presents the generalization of the PSM formulation for any flow regimes. In Section 4 the implications of the PSM predictions are discussed. Materials and methods adopted in the experiments are described in Section 5 and all validation steps are presented in Section 6.

2. Hydrodynamic force on a particle immersed in a bi-disperse suspension

In the Particle Segregation Model the segregation direction results from a balance of the hydrodynamic force and gravity on a single particle in the mixture. The critical element in the balance is the drag force exerted by the fluid in a bi-disperse suspension (Di Maio et al., 2012). The formulation of accurate and generally valid expressions for the local fluid-particle interaction has always stimulated research efforts. In particular, account for the effects of polydispersity of the suspension on the drag force acting upon a specific particle is receiving special attention. Various expressions for such force have been proposed (Van der Hoef et al., 2005; Holloway et al., 2009; Yin and Sundaresan, 2009; Cello et al., 2010) and simulations seem to confirm their validity (Beetstra et al., 2007; Di Renzo et al., 2011). Here, we propose a formulation that overcomes the limitations of viscous-flow conditions with respect to previous attempts (Di Maio et al., 2012; Di Renzo et al., 2012).

The total interaction force N experienced by a particle of a bed is typically subdivided for convenience into a pressure gradient term and a *pure* drag force F:

$$N = V\left(-\frac{dp}{dz}\right) + F \tag{1}$$

in which V is the particle volume, p is the fluid *net* pressure (i.e. free from the hydrostatic contribution, see e.g. Cello et al., 2010), and z is the vertical coordinate.

Consider a uniform mixture of kt monodisperse solids species, namely the bed components. Under fully-developed, steady-state flow conditions, the relation between the overall pressure drop across

the bed and the drag force on individual particles can be expressed as the sum of each component's weighted contribution (Cello et al., 2010), i.e.:

$$-\frac{dp}{dz} = \frac{6(1-\varepsilon)}{\pi} \sum_{k=1}^{kt} \frac{x_k N_k}{D_k^3} \tag{2}$$

where x_k is the volumetric fraction of the species k and ε is bed voidage. In analogy with the monodisperse case, the overall pressure drop across the bed can be referred to an average particle-scale force, to be calculated at an appropriate average diameter, i.e.:

$$-\frac{dp}{dz} = \frac{6(1-\varepsilon)}{\pi} \frac{\overline{N}}{\overline{D}^3} \tag{3}$$

This simply corresponds to introducing the two average variables, and it is always possible to find a suitable definition of one quantity, typically the diameter, and derive the definition of the other one.

As a convenient measure of the size dispersion in relation to species i, the polydispersion index proposed by van der Hoef et al. (2005) is recalled:

$$y_i = \frac{D_i}{\overline{D}} \tag{4}$$

It is now postulated that the force experienced by a particle in the mixture can be expressed in terms of the average force:

$$N_k = \alpha_k \overline{N} \tag{5}$$

i.e. by introducing the dimensionless force specification coefficients α_k.

By substituting Eq. (5) into Eq. (2) and equating the overall pressure drop to Eq. (3), one obtains a constraint on the definitions involved to guarantee model consistency, i.e.:

$$\sum_{k=1}^{kt} \frac{x_k \alpha_k}{y_k^3} = 1 \tag{6}$$

Note that by setting $\alpha_k = y_k^3$ Eq. (6) is trivially fulfilled. Other possible expressions for α_k are related to the definition of the average diameter $\overline{D}$ and can include the polydispersion index y as well as the voidage.

An appropriate average diameter is Sauter's definition (Gibilaro et al., 1986):

$$\overline{D} = \left(\sum \frac{x_k}{D_k} \right)^{-1} \tag{7}$$

This leads to another possibility for the specification coefficient, named $\alpha_k = y_k^2$. Furthermore, any linear combination of the kind:

$$\alpha_k = a y_k^2 + (1-a) y_k^3 \tag{8}$$

where a is a coefficient to be defined, is in fact consistent with Eq. (6).

Similar considerations and derivations apply if the problem is formulated in terms of pure drag force F instead of N. Specification coefficients are introduced as:

$$F_k = \beta_k \overline{F} \tag{9}$$

with the requirement that $\overline{F} = \varepsilon \overline{N}$ and

$$\sum_{k=1}^{kt} \frac{x_k \beta_k}{y_k^3} = 1 \tag{10}$$

so that a plausible expression for β_k is

$$\beta_k = b y_k^2 + (1-b) y_k^3 \tag{11}$$

where b is another coefficient to be defined.

A direct comparison of the expressions for F_k and N_k leads to the following two relations, one between the two forces:

$$F_k = \varepsilon \frac{\beta_k}{\alpha_k} N_k \tag{12}$$

and one between the specification coefficients:

$$\alpha_k = \beta_k \varepsilon + (1-\varepsilon) y_k^3 \tag{13}$$

Amongst the many possibilities, three examples of compatible formulations of the specification coefficients are listed in Table 1.

In order to discriminate between the possibilities, considerations on an extreme case appear useful. Let us analyse the force experience by a single, very large particle immersed in a fluidized bed of

fine material. Let us denote bed material with index 1 and the particle with index 2. It is known and well documented that the particle will be in equilibrium when its density ρ_2 equals the bulk density of the suspended bed $\rho_1(1-\varepsilon)$ (see e.g. Kunii and Levenspiel, 1991). The above concept can be cast in form of a balance of the net force acting on the sphere and its weight:

$$\alpha_2 \overline{N} = \rho_2 \frac{\pi D_2^3}{6} g \tag{14}$$

whence we shall derive the density ρ_2 of the sphere that is in equilibrium with the fluidized bed. If the particle is just one and very large we have that $D_1/D_2 \to 0$, $x_1 \to 1$, $\overline{D} \to D_1$ and $y_2 \to D_2/D_1$. In the bed the average net force assumes the value necessary to support the weight of a fine particle. Thus, invoking also the coefficient *a*, we get:

$$\left[a\left(\frac{D_2}{D_1}\right)^2 + (1-a)\left(\frac{D_2}{D_1}\right)^3\right]\rho_1 \frac{\pi D_1^3}{6} g = \rho_2 \frac{\pi D_2^3}{6} g \tag{15}$$

whence, after simple manipulations and using the vanishing size ratio:

$$\rho_2 = \rho_1(1-a) \tag{16}$$

The obvious correct choice is then $a = \varepsilon$, corresponding to case 1 in Table 1, leading to:

$$\varepsilon y_k^2 + (1-\varepsilon) y_k^3 \tag{17}$$

The definition of the specification coefficients allows calculating the ratio of drag forces for the two particle species. Owing to the fact that such ratio is in fact the ratio of the specification coefficients, its dependence on the size ratio and other variables is different depending on the drag force considered. Fig. 2 shows the plots of the pure and net drag forces versus the size ratio. While the pure drag force ratio scales only with the square of the size ratio (Fig. 2a), that of the net forces exhibits a dependence, though very limited, on composition – through the average diameter – and voidage (Fig. 2b). All net force ratio curves in Fig. 2b lay between the quadratic and cubic dependence on size ratio. The results demonstrate that the two forces, both sometimes equivocally called "drag force", are indeed conceptually different. Analyses of the effect of using different drag laws for binary mixtures (like in e.g. Okayama et al., 2006; Zhou and Yu, 2009) require special care to avoid any possible confusion.

The reader will note that the result found for α_k in Eq. (17) (Case 1 in Table 1) corresponds to the expression derived, under the assumption of viscous flow, by van der Hoef et al. (2005). The

difference is that in the present derivation no specific flow regime was required. The agreement in validation tests for slight modifications of the above-mentioned model in random bidisperse arrays computed by lattice-Boltzmann simulations (Van der Hoef et al., 2005; Sarkar et al., 2009) and for the layer inversion phenomenon in liquid-fluidized beds by DEM-CFD simulations (Di Renzo et al., 2011) provides an indirect confirmation of the sound physical basis of the approach. However, further elaborations by comparison of results at the macroscopic scale with experimental results are required, some of which are discussed below.

3. Generalization of the particle segregation model (PSM)

The particle segregation model (PSM) is based on the balance of the gravitational and hydrodynamic forces acting on a single particle immersed in a fluidized bed of two solids. In our previous work (Di Maio et al., 2012), the model was described for the case of a single particle immersed in a bed of a different fluidized suspension and for binary mixtures. However, discussion was limited to the viscous flow regime. After a summary of the model foundations, we will show that the general specification coefficients described in Section 2 along with expressions for the average drag force valid for any flow regime allow overcoming the limitation to low-Reynolds' number flows.

In the case of a gas-fluidized binary mixture composed of species 1 and species 2, we propose to set the force balance on one particle of species 2, by convention the bigger particle. Model assumptions are as follows:

a. bed is composed of two fully mixed spherical solids;

b. binary bed is in the fluidized state, i.e. the total sum of the hydrodynamic forces exerted by the fluid equals the total bed weight;

c. voidage is uniform.

The model is based on a rather elementary concept (Di Maio et al., 2012), named that each particle in the bed is subjected to the action of gravity and momentum transfer by the fluid, which may be unbalanced. Indeed, it should be noted that assumption (b) apply to the bed as a whole and it does not imply that *each* particle, taken individually, is at equilibrium with respect to drag and gravity. It is fully compliant with the hypotheses that the particles belonging to one species exhibit domination of drag over gravity and the reverse occurs for particles belonging to the other species. Therefore, eventually the force balance on the test particle would indicate whether it, and all particles of the

same species, will be pushed upwards by the action of the fluid or will tend to sink to the bottom as a result of the dominance of weight.

Because of assumption (b) the pressure gradient developing across the bed can be expressed in terms of the bulk density of the binary suspension as:

$$-\frac{dp}{dz} = \overline{\rho}(1-\varepsilon)g \tag{18}$$

where

$$\overline{\rho} = \rho_1 x_1 + \rho_2(1-x_1) \tag{19}$$

As far as the drag force is concerned, it is necessary to apply Eq. (9) at the velocity necessary to suspend the emulsion phase of the (mixed) binary bed, i.e. the minimum fluidization velocity $\overline{u}_{mf}$ of an equivalent solid of density $\overline{\rho}$ and diameter $\overline{D}$. In our previous derivation (Di Maio et al., 2012), the hypothesis of viscous flow led to the following formula for the pure drag force on the particle of species 2 at the relevant velocity:

$$F_2\big|_{u=\overline{u}_{mf}} = \frac{1}{6}\pi g \varepsilon \overline{\rho}\,\overline{D} D_2^2 \tag{20}$$

However, it is straightforward to show that the above relation holds for any given dependence of the force on the velocity, e.g. using expressions derived from Ergun's pressure drop (Ergun, 1952) or Di Felice's formula (Di Felice, 1994). In fact, making use of the equivalence between the net drag force and weight of the average species, evaluation of the above force in more general terms is obtained by:

$$F_2\big|_{u=\overline{u}_{mf}} = y_2^2 \overline{F}\Big|_{u=\overline{u}_{mf}} = y_2^2 \varepsilon \overline{N}\Big|_{u=\overline{u}_{mf}} = y_2^2 \varepsilon \overline{\rho}\frac{\pi \overline{D}^3}{6} g = \frac{1}{6}\pi g \varepsilon \overline{\rho}\,\overline{D} D_2^2 \tag{21}$$

without the assumption of a particular flow regime or drag expression.

The condition for the test particle to be pushed upwards arises from the comparison of the net fluid-particle force, as evaluated in Eq. (1), at the minimum fluidization velocity of the mixture and the particle's weight, as follows:

$$V_2 \overline{\rho}(1-\varepsilon)g + \tfrac{1}{6}\pi g \varepsilon \overline{\rho}\,\overline{D} D_2^2 > V_2 \rho_2 g \tag{22}$$

By introducing the following density and size ratios:

$$\bar{s} = \frac{\rho_2}{\bar{\rho}} \tag{23a}$$

$$\bar{d} = \frac{\bar{D}}{D_2} \tag{23b}$$

Eq. (22) reduces simply to

$$\bar{s} < 1 - \varepsilon + \varepsilon \bar{d} \tag{24}$$

It is convenient to express the above ratios also in terms of the corresponding species properties, giving:

$$\bar{s} = \left(\frac{x_1}{s} + 1 - x_1 \right)^{-1} \tag{25a}$$

$$\bar{d} = \left(\frac{x_1}{d} + 1 - x_1 \right)^{-1} \tag{25b}$$

where

$$s = \frac{\rho_2}{\rho_1} \tag{26a}$$

$$d = \frac{D_1}{D_2} \tag{26b}$$

Eq. (24) can include the equilibrium dictated by the equality and be expressed in terms of s and d, yielding:

$$s \leq \frac{(1-\varepsilon)(1-d)x_1 + d}{(1-x_1)(d+\varepsilon-\varepsilon d) + x_1} \tag{27}$$

Summarizing the above derivation, we have that given solids properties and bed composition Eq. (27) allows predicting whether species 2 will tend to be pushed upwards, i.e. act as flotsam (if the inequality is satisfied), or settle to the bottom, representing the jetsam in the mixture (if the opposite inequality applies).

It shall be remarked that only the initial tendency is currently predictable through the PSM, while no information is provided on the extent of the segregation at the end of the process, i.e. its steady-state "intensity".

3.1 Individual minimum fluidization velocities

It is interesting to try to relate the results expressed by Eq. (27) and the minimum fluidization velocities of the individual bed components. In fact, in the past their values determined the role of *fluidized* and *packed* attribute to the mixture components (Chiba et al., 1980).

Let us focus on the simplified condition of complete segregation of the two components, a system where the individual u_{mf} represent directly the relevant velocities, i.e. there is no interaction of the two solids on their fluidization behavior. Under this circumstance, the two solids may be regarded simply as two monocomponent beds one on top of the other.

Indications on the suspended component in the bed will therefore be obtained by comparing the two minimum fluidization velocities. Assuming uniform voidage and the same flow regime throughout the bed, the conditions for the two solids to have the same minimum fluidization velocity can be expressed by:

$$\rho_1 D_1^2 = \rho_2 D_2^2 \qquad \text{(viscous regime)} \tag{28}$$

$$\rho_1 D_1 = \rho_2 D_2 \qquad \text{(inertial regime)} \tag{29}$$

which, in terms of the dimensionless variables introduced, become:

$$s = d^2 \qquad \text{(viscous regime)} \tag{30}$$

$$s = d \qquad \text{(inertial regime)} \tag{31}$$

By comparing Eqs. (30-31) and Eq. (27) we found that the condition of equal u_{mf} of the pure components does not correspond to the equilibrium of forces when the two solids are mixed. The two results appear rather independent and can therefore be used distinctly for the segregation, the former, and the fluidization, the latter, respectively.

4. Model predictions

4.1 Segregation direction from the PSM

The condition prescribed by Eq. (27) relating the density and size ratios, voidage and composition is the main result of the Particle Segregation Model and is shown here to be independent of the flow regime. Equilibrium conditions result as shown, in terms of components' density and size ratio from Eq. 27, in Fig. 3a and, in terms of component-to-average density and size ratio from Eq. 24, in Fig. 3b. Note that explicit dependence of the bed composition appears in Fig. 3a, while a unique master

curve is obtained, for a given voidage, when the ratios involve the average properties, Fig. 3b. It is the case to mention that the influence of voidage values is relatively modest, as changes within the range of interest for mixtures (e.g. between say 0.3 and 0.4) cause only slight displacements of the curves in the plots of Fig. 3, as it can be easily verified using Eqs. (24) or (27).

Considerations on the inequality allow identifying characteristic segregation patterns. Fig. 3 shows how the chart is subdivided into a lower zone, in which the bed tend to segregate with the LB component acting as flotsam, and an upper zone, in which the role of flotsam is played by the HS component. When using Fig. 3a, the reader will notice that the limit curve discriminating zones with different segregation direction is the one corresponding to the overall volume composition x_1 in the bed.

4.2 Segregation/fluidization patterns

A plot of the results of Eq. (30) and (31) on the *s*-*d* diagram allows completing the characterization of the expectable scenarios, as predicted by the combination of the PSM and the comparison of the pure components' minimum fluidization velocities in the complete segregation case (Fig. 4). Diagrams showing the viscous and inertial regime cases are shown in Figs. 4a and 4b, respectively. Note that a distinct plot is necessary for the two flow regimes only because of the difference in the equal minimum fluidization conditions.

For property ratios belonging to the lower part of the plot (zone A in Fig. 4) the systems is predicted to evolve by segregating the less dense component towards the top of the bed, which consequently undergoes free fluidization on top of the rest of the bed.

Under combinations of densities and sizes belonging to the middle zone of Fig. 4 (zone B), i.e. above the equal u_{mf} curve and below the equilibrium line at the given system composition, the initially mixed system evolves in the same segregation direction as the previous case. However, in this case the segregated component that would be (if pure) over-fluidized is the HS species, which tends to settle to the bottom of the bed. Therefore, this would be fluidized below the stagnant rest of the bed.

If the density ratio is not very different from unity and size difference is sufficiently large (zone C in Fig. 4), a binary mixture is predicted to tend to segregate with the denser component (fluidized) at the top of the bed. Thus, above equilibrium lines the denser component tends to act as flotsam in the mixture. In this case, the system exhibits fluidization of the HS species on top of the rest of the bed.

In summary, the combination of the results of the particle segregation model, Eq. (27), and the equal minimum fluidization condition, Eq. (30) or (31), establish the basis for a theoretically sound framework for the characterization of the segregation tendency of complex mixtures. As introduced elsewhere (Di Maio et al., 2012) and extended below, experimental findings appeared in the literature do not contradict the picture described above.

5. Experimental method

Specific experiments have been carried out in an attempt to focus the attention on the behavior of material pairs endowed with properties falling in particular areas of the *s*-*d* plane. All other experimental data were collected from tests in a 10-cm ID transparent cylindrical fluidization column, equipped with a 4-mm-thick plastic porous distributor. The experimental procedure is as follows. Starting from a well-mixed packed bed, whose homogeneity has been ensured by slowly pouring several mechanically pre-mixed portions of the total solid mass (Formisani et al., 2011), the fluidizing air flow was increased up to a velocity value slightly above the minimum fluidization velocity of the mixture. In order to obtain data relevant to the concentration profile along the column, the "freezing" procedure was applied, as documented by various authors (Rowe and Nienow, 1976; Nienow et al., 1978; Chiba et al., 1979, 1980; Beeckmans and Stahl, 1987; Čársky et al., 1987; Hoffmann et al., 1993; Wu and Baeyens, 1998; Formisani et al., 2001, 2008a, 2008b). To this regard a valve on the feed line was employed to suddenly cut the air flow off; afterwards, horizontal layers of particles were drawn from the top of the column, separated by sieving and weighted. The concentration profile was used to determine univocally the segregation direction.

In addition to tests in the cylindrical set-up, qualitative observations have been conducted visually in a 2D transparent fluidization set-up (15 cm by 1.5 cm cross-sectional area and porous-plate distributor), whose results are reported and discussed in Section 6.1.

Measurements involved four types of closely sieved, nearly spherical solids: glass ballotini (GB), molecular sieves (MS), steel shots (SS), bronze shots (BS) and zirconium silicate spheres (ZS). Their properties are listed in Table 2. From these cuts, the four mixtures listed in Table 3 have been prepared. In all experiments, the component masses were adjusted so to ensure a packed bed aspect ratio initially set equal to 1.7.

The segregating behavior of three GB-MS mixtures has been experimentally investigated at various size ratios, keeping the component volume fraction $x_1 = 0.5$. The effect of composition has been addressed for the GB162-MS824 bed. The choice of the mixture BS70-SS229 has been aimed at

producing data in a region of the *s*-*d* plane where the availability of experiments in the literature is scarce. Finally, an additional binary bed was examined, ZS168-GB898, whose component size ratio is similar to another GB-MS system.

6. Comparison of predictions and measurements

6.1 Observation of type B segregation patterns

Of the four extreme segregation types discussed in Section 1, type A is the most commonly encountered one. As already mentioned, behavior ascribable to type C was also previously reported and classified, mostly as an exception. Fluidization below a packed bed, such as typical of cases B and D, is much more difficult to conceive. In an attempt to observe type B segregation, a mixture of bigger glass ballotini (D = 570 μm) and smaller steel shots (D = 229 μm), initially mixed, was fluidized in the 2D rig to highlight the presence of a top- or bottom-localized bubbling. With reference to Fig. 4a, the mixture (d = 0.40 and s = 0.33) falls inside the zone whose corresponding extreme segregation pattern is type B. Visual observation of the fluidization process, in fact, confirmed the presence of a bed composed of a lower bubbling layer and an upper packed layer (Fig. 5). In Fig. 5a-5c a sequence of three photographs of the observed behavior are reported. The mixture did not segregate completely, but a clear interface where bubbles ended up "absorbed" was distinctly visible. With respect to the pre-fluidization stage, the system appeared segregated, though not completely, and fully at suspension, i.e. with the gas pressure drop balancing the bed weight. In order to allow for the formation and growth of bubbles the initial mixture lifted slightly, while at the same time material from the bottom of the bed fell, undergoing fluidization and separation. However, since this transient detachment did not involve the entire mass up to the surface, the upper portion of the bed eventually remained supported by the bubbling bed. As a final note, it is remarked that the process resulted fully stable, in the sense that no further evolution was observed after hours of operation under the conditions shown in Fig. 5. Repeated trials in the same apparatus and experiments in the 3D column showed no qualitative differences. It is the case to mention that the presented observations are also in line with those reported by Formisani et al. (Formisani et al., 2012), who denoted such behavior as *bottom fluidization* vs. the most common *top fluidization*.

Conditions with the LB solid fluidizing below a packed bed composed mostly of the HS species, i.e. type D segregation, as hypothesized in Section 1 (Fig. 1d), was neither predicted by the model nor observed in any experiments, and can likely be considered as not plausible.

6.2 Very large particles in a fluidized bed

A first way to examine the predicting capabilities of the PSM is to compare the segregation direction with the experimentally observed prevalence of individual spheres in the upper region or in the lower region of a fluidized bed of fine particles. A useful experimental analysis of this kind was conducted by Oshitani et al. (2004). They investigated the tendency of a relatively small amount of large particles of relatively low density to appear towards the surface or the bottom of a vibro-fluidized bed of fine (and denser) glass ballotini. Data extracted from the work along with the corresponding model predictions are reported in Table 4. In the experiments 6-Nylon spheres tend to float over the bed for the entire range of sphere diameters investigated, while the Teflon sphere tends to sink for all sizes of the bed particles. Model predictions agree in all reported cases, demonstrating the capability to discriminate even between two systems relatively similar in s and d ratios but exhibiting a different segregation direction, named System 1 and System 6 in Table 4.

6.3 Segregation direction in binary fluidized beds

A review of the experimental findings available in the literature on gas-fluidized binary beds with the sought properties revealed a significant number of works, although often with a variable extent of the details reported. Most of the systems were present already in our previous comparisons (Di Maio et al., 2012; Di Renzo et al., 2012), except the ones characterized by higher particle Reynolds number. The properties of all the collected systems (53 systems from 15 different references) are listed in Table 5, together with the 7 systems investigated in the present work and detailed in Section 5. Note that the vast majority of them exhibit the LB solid as flotsam, some of them are characterized by a change of the flotsam component with bed composition and few systems appear with the HS species acting as flotsam. Table 5 also contains the predictions of the PSM as regards the segregation direction, with specific computation for different compositions whenever the experimental datum was not available.

All systems are plotted in Fig. 6 along with the equilibrium curve prescribed by the PSM. Note that each point represents values of $\bar{s}$ and $\bar{d}$, as determined by the size and density ratios of the solids, namely s and d, and bed composition (Eq. 26). In the plot, the behavior exhibited is represented using different symbols depending upon the type of segregating system observed: big open symbols are used to denote conditions where the LB species is flotsam, small solid circles when the HS species is flotsam and crosses when the system is reported as mixed. The straight line denotes the equilibrium of the tendencies as prescribed by the PSM (Eq. 24), so it discriminates between the two segregation directions. Fig. 6 and Table 5 show that the separation of behavior predicted by the

PSM corresponds to the experimental observations for a very broad range of different solids combinations and operating conditions. Exceptions to the proposed rule occur in few cases where the separation direction component is reversed with respect to the predictions and in those cases where bed mixing is observed. As reported in Table 5, for some binary mixtures data are available at different bed compositions, of particular importance being those where a corresponding change of behavior is observed. In order to examine the effect of a change of composition in Fig. 6 for a given solid pair, it is useful to note that average ratios $\bar{s}$ and $\bar{d}$ change according to Eqs. 25a-b. In particular, they both tend to unity as x_1 tends to zero and they tend to the corresponding values s and d as x_1 tends to one. Therefore, the location of the point moves as bed composition varies. Now, if the model predictions are correct, then curves corresponding to binaries segregating always in the same direction should be located entirely on one side of the equilibrium line, while those representing pairs exhibiting a reversal should cross the PSM line. Fig 7 shows such curves along with symbols, using the same convention as in Fig. 6, corresponding to experimental measurements for selected systems. Fig. 7a shows the comparison of predictions and observations in cases of constant segregation direction (LB is flotsam), while Figs. 7b-d show three cases in which a change of behavior is observed. For the system examined by Formisani et al. (2008a) (Fig. 7b), the unusual behavior (HS species as flotsam) is reported at lower values of x_1 while the bed tends to mix at higher concentrations. The model also predicts a change of behavior with composition, although a sharper one directly to the opposite segregation direction, for a composition compatible with the experiments. For the system reported in Chiba et al. (1980), the curve representing different compositions of the examined solids pair is also shown to cross the equilibrium curve (Fig. 7c). However, the predicted composition corresponding to the change of the direction results higher than the experimentally observed value. The third mixture, examined in the present work, exhibits a change of segregation pattern at the cross with the equilibrium line (Fig. 7d). In the experiments, the segregation intensity observed in both directions appeared modest and the bed could have also been judged essentially mixed at all compositions, with a slight tendency of either species to float to the surface in the two more "extreme" compositions.

It is worth noting that, despite the relatively coarse approximations of the model, the simplicity of the obtained relations and the lack of adjustable parameters, in all cases where segregation inversion or, at least a change of behavior, was observed in experiments, the corresponding curves cross the model line on the $\bar{s}$-$\bar{d}$ chart. On the other hand, inclination of such curves with respect to the equilibrium line is low, so that small changes in the variables (e.g. due to inaccurate average sizes or significant polydispersion, uncertainties of the voidage value and its dependence on composition)

may result in significant influence on the accuracy of the predictions, partly justifying the difficulties in catching the exact critical values.

Also, it should not be forgotten that the initial fluidization process (i.e. the transition from the fixed to the fluidized bed with gas velocity) for a mixture is not an on-off process and it is not infrequent that below or above the suspended part of bed, solids become packed again as a result of the transient and possibly limited segregation process. After such changes in the local bed composition the model predictions can no longer be considered applicable, at least on the global scale. Therefore, the model predictions shall be intended only as initial segregation direction starting from a mixed bed.

In summary, also in consideration of the fact that no relations had previously proposed to predict the tendency toward the correct segregation pattern, the discrimination between the two segregation directions predicted by the PSM appears in good agreement with the available data. Additional verification of the predicted tendency and possibly to its reversal with bed composition is necessary to further assess the validity of the proposed model in more general terms.

7. Conclusions

The segregating behavior of components in a gas-fluidized mixture of solids was studied by means of a generalization of the recently proposed Particle Segregation Model (PSM) and the consideration of the minimum fluidization velocity of the mixture constituents. The focus was on the characterization of the segregation patterns of pairs of a small-denser species (HS) and a big-less-dense species (LB) at incipient fluidization, although the results can be extended to other, more trivial, cases. The PSM involves careful evaluation of the drag and buoyancy forces and is based on balances at the particle scale. Coefficients of the force repartition between differently sized particle species are derived in general terms and force dependence on the size ratio is analyzed for the pure drag force (i.e. excluding pressure gradient) and the net force (including pressure gradient) formulations. On this basis, the first result of this work is that the PSM proves valid more in general than previously reported, as the extension to all flow regimes is possible without model modifications. Coupled to the equal minimum fluidization condition, the segregation direction predictions of the PSM allow defining a map of three possible segregation/fluidization scenarios, observable depending upon the combinations of size ratio, density ratio and mixture composition:

1. HS particles segregating at the bottom and LB particles to the top, with the latter being fluidized, for $s < d^2$ in the viscous flow regime and $s < d$ in the inertial regime;

2. HS particles segregating at the bottom and LB particles to the top, with the former being fluidized below a stagnant bed containing the rest of the mixture, for $s > d^2$ or $s > d$ (for viscous and inertial regime, respectively) and s below the (composition dependent) equilibrium curve prescribed by Eq. (27);

3. HS particles segregating and fluidizing at the top of the bed for s above the equilibrium curve prescribed by Eq. (27).

Comparison of model predictions and experiments is carried out in different ways. The occurrence of the most unexpected behavior predicted by the model, i.e. a partially segregated bed fluidized from below (and stagnant at the top), is demonstrated in a 2D setup and also reproduced in 3D columns. Predictions of the tendency to float or sink of very large spheres immersed in a fluidized bed were validated with experimental data available in the literature. Finally, the capabilities of the PSM to prescribe the segregation tendency or "direction" of binary mixtures were assessed by comparison with an extensive set of measurements including 53 systems available in the literature and 7 systems examined in this work. Of particular relevance is the demonstration of the capability to catch, with a reasonable accuracy, change of segregation behavior for the same mixture with bed composition. Further investigations are required to verify the condition of mixing (at low velocity) suggested by the PSM results for systems characterized by properties in the vicinity of the equilibrium curves.

List of symbols

D	particle diameter, m
$\overline{D}$	Sauter's mean particle diameter, m
d	diameter ratio (D_1/D_2), -
$\bar{d}$	average diameter ratio ($\overline{D}/D_2$), -
F_d	pure drag force, N
g	gravitational acceleration, m/s^2
N	net fluid-particle interaction force, N
$\overline{N}$	spatially averaged net fluid-particle force, N
p	*net* pressure, Pa
$\overline{Re}$	average Reynolds number, -
s	inverse density ratio (ρ_2/ρ_1), -
$\bar{s}$	inverse average density ratio ($\rho_2/\bar{\rho}$), -
u	superficial fluid-to-particle relative velocity, m/s
u_{mf}	minimum fluidization velocity, m/s
$\bar{u}_{mf}$	average minimum fluidization velocity, m/s
V_p	particle volume, m^3
x	fluid-free solids volumetric fraction, -
y	polydispersion index $y_i = D_i/\overline{D}$, -
z	vertical coordinate, m

Greek symbols

α	species-to-average net fluid-particle force ratio, -
β	species-to-average pure drag force ratio, -
ε	voidage, -
μ	fluid viscosity, Pa·s
ρ	solid density, kg/m^3
$\bar{\rho}$	average solid density, kg/m^3
ρ_f	fluid density, kg/m^3

Subscripts

1, 2	index for solid species
Exp	experiments
i, *j*	relative to the *i*-th, or *j*-th particle or particle species
Sim	simulations

Acronyms

LB	Bigger-less-dense species
PSM	Particle Segregation Model
HS	Smaller-denser species

References

Beeckmans, J.M., Stahl, B., 1987. Mixing and segragation kinetics in a strongly segregated gas-fluidized bed. Powder Technology 53, 31–38.

Beetstra, R., Van der Hoef, M.A., Kuipers, J.A.M., 2007. Numerical study of segregation using a new drag force correlation for polydisperse systems derived from lattice-Boltzmann simulations. Chemical Engineering Science 62, 246–255.

Bokkers, G.A., Van Sint Annaland, M., Kuipers, J.A.M., 2004. Mixing and segregation in a bidisperse gas–solid fluidised bed: a numerical and experimental study. Powder Technology 140, 176–186.

Cello, F., Di Renzo, A., Di Maio, F.P., 2010. A semi-empirical model for the drag force and fluid–particle interaction in polydisperse suspensions. Chemical Engineering Science 65, 3128–3139.

Chao, Z., Wang, Y., Jakobsen, J.P., Fernandino, M., Jakobsen, H.A., 2012. Multi-fluid modeling of density segregation in a dense binary fluidized bed. Particuology 10, 62–71.

Chiba, S., Chiba, T., Nienow, A.W., Kobayashi, H., 1979. The minimum fluidisation velocity, bed expansion and pressure-drop profile of binary particle mixtures. Powder Technology 22, 255–269.

Chiba, S., Nienow, A.W., Chiba, T., Kobayashi, H., 1980. Fluidised binary mixtures in which the denser component may be flotsam. Powder Technology 26, 1–10.

Cui, H., Grace, J.R., 2007. Fluidization of biomass particles: A review of experimental multiphase flow aspects. Chemical Engineering Science 62, 45–55.

Dahl, S.R., Hrenya, C.M., 2005. Size segregation in gas–solid fluidized beds with continuous size distributions. Chemical Engineering Science 60, 6658–6673.

Di Felice, R., 1994. The voidage function for fluid-particle interaction systems. International Journal of Multiphase Flow 20, 153–159.

Di Maio, F.P., Di Renzo, A., Vivacqua, V., 2012. A particle segregation model for gas-fluidization of binary mixtures. Powder Technology 226, 180–188.

Di Renzo, A., Cello, F., Di Maio, F.P., 2011. Simulation of the layer inversion phenomenon in binary liquid--fluidized beds by DEM–CFD with a drag law for polydisperse systems. Chemical Engineering Science 66, 2945–2958.

Di Renzo, A., Di Maio, F.P., Girimonte, R., Formisani, B., 2008. DEM simulation of the mixing equilibrium in fluidized beds of two solids differing in density. Powder Technology 184, 214–223.

Di Renzo, A., Di Maio, F.P., Vivacqua, V., 2012. Prediction of the Flotsam Component in a Gas-Fluidized Bed of Two Dissimilar Solids. International Journal of Chemical Reactor Engineering 10, A26.

Ekinci, E., Atakül, H., Tolay, M., 1990. Detection of segregation tendencies in a fluidised bed using temperature profiles. Powder Technology 61, 185–192.

Ergun, S., 1952. Fluid flow through packed columns. Chemical Engineering Progress 48, 89–94.

Feng, Y.Q., Xu, B.H., Zhang, S.J., Yu, A.B., Zulli, P., 2004. Discrete particle simulation of gas fluidization of particle mixtures. AIChE Journal 50, 1713–1728.

Feng, Y.Q., Yu, A.B., 2007. Microdynamic modelling and analysis of the mixing and segregation of binary mixtures of particles in gas fluidization. Chemical Engineering Science 62, 256–268.

Formisani, B., De Cristofaro, G., Girimonte, R., 2001. A fundamental approach to the phenomenology of fluidization of size segregating binary mixtures of solids. Chemical Engineering Science 56, 109–119.

Formisani, B., Girimonte, R., Longo, T., 2008a. The fluidization process of binary mixtures of solids: Development of the approach based on the fluidization velocity interval. Powder Technology 185, 97–108.

Formisani, B., Girimonte, R., Longo, T., 2008b. The fluidization pattern of density-segregating binary mixtures. Chemical Engineering Research and Design 86, 344–348.

Formisani, B., Girimonte, R., Vivacqua, V., 2011. Fluidization of mixtures of two solids differing in density or size. AIChE Journal 57, 2325–2333.

Formisani, B., Girimonte, R., Vivacqua, V., 2012. Fluidization of mixtures of two solids: A unified model of the transition to the fluidized state. AIChE Journal n/a–n/a.

Gera, D., Syamlal, M., O'Brien, T.J., 2004. Hydrodynamics of particle segregation in fluidized beds. International Journal of Multiphase Flow 30, 419–428.

Gibilaro, L.G., Di Felice, R., Waldram, S.P., Foscolo, P.U., 1986. A predictive model for the equilibrium composition and inversion of binary-solid liquid fluidized beds. Chemical Engineering Science 41, 379–387.

Gibilaro, L.G., Rowe, P.N., 1974. A model for a segregating gas fluidised bed. Chemical Engineering Science 29, 1403–1412.

Gilbertson, M.A., Eames, I., 2001. Segregation patterns in gas-fluidized systems 433, 347–356.

Hoffmann, A.C., Janssen, L.P.B.M., Prins, J., 1993. Particle segregation in fluidised binary mixtures. Chemical Engineering Science 48, 1583–1592.

Holloway, W., Yin, X., Sundaresan, S., 2009. Fluid-particle drag in inertial polydisperse gas-solid suspensions. AIChE Journal 56, 1995–2004.

Hoomans, B.P.B., Kuipers, J.A.M., Van Swaaij, W.P.M., 2000. Granular dynamics simulation of segregation phenomena in bubbling gas-fluidised beds. Powder Technology 109, 41–48.

Huilin, L., Yurong, H., Gidaspow, D., 2003. Hydrodynamic modelling of binary mixture in a gas bubbling fluidized bed using the kinetic theory of granular flow. Chemical Engineering Science 58, 1197–1205.

Jang, H.T., Park, T.S., Cha, W.S., 2010. Mixing–segregation phenomena of binary system in a fluidized bed. Journal of Industrial and Engineering Chemistry 16, 390–394.

Joseph, G.G., Leboreiro, J., Hrenya, C.M., Stevens, A.R., 2007. Experimental segregation profiles in bubbling gas-fluidized beds. AIChE Journal 53, 2804–2813.

Kunii, D., Levenspiel, O., 1991. Fluidization Engineering. Butterworth-Heinemann, Boston.

Marzocchella, A., Salatino, P., Di Pastena, V., Lirer, L., 2000. Transient fluidization and segregation of binary mixtures of particles. AIChE Journal 46, 2175–2182.

Mazzei, L., Casillo, A., Lettieri, P., Salatino, P., 2010. CFD simulations of segregating fluidized bidisperse mixtures of particles differing in size. Chemical Engineering Journal 156, 432–445.

Naimer, N.S., Chiba, T., Nienow, A.W., 1982. Parameter estimation for a solids mixing|segregation model for gas fluidised beds. Chemical Engineering Science 37, 1047–1057.

Nienow, A.W., Rowe, P.N., Cheung, L.Y.-L., 1978. A quantitative analysis of the mixing of two segregating powders of different density in a gas-fluidised bed. Powder Technology 20, 89–97.

Okayama, Y., Doi, A., Kawaguchi, T., Tanaka, T., Tsuji, Y., 2006. Drag Force Model for Fluidized Bed of Binary Mixture of Particles, in: Proceedings of the 5th World Congress on Particle Technology.

Olivieri, G., Marzocchella, A., Salatino, P., 2004. Segregation of fluidized binary mixtures of granular solids. AIChE Journal 50, 3095–3106.

Olivieri, G., Marzocchella, A., Salatino, P., 2009. A fluid-bed continuous classifier of polydisperse granular solids. Journal of the Taiwan Institute of Chemical Engineers 40, 638–644.

Oshitani, J., Ono, K., Ijiri, M., Tanaka, Z., 2004. Effect of particle fluidization intensity on floating and sinking of objects in a gas–solid fluidized bed. Advanced Powder Technology 15, 201–213.

Owoyemi, O., Mazzei, L., Lettieri, P., 2007. CFD modeling of binary-fluidized suspensions and investigation of role of particle-particle drag on mixing and segregation. AIChE Journal 53, 1924–1940.

Qiaoqun, S., Huilin, L., Wentie, L., Yurong, H., Lidan, Y., Gidaspow, D., 2005. Simulation and experiment of segregating/mixing of rice husk–sand mixture in a bubbling fluidized bed. Fuel 84, 1739–1748.

Rao, A., Curtis, J.S., Hancock, B.C., Wassgren, C., 2011. Classifying the fluidization and segregation behavior of binary mixtures using particle size and density ratios. AIChE Journal 57, 1446–1458.

Rasul, M.G., Rudolph, V., 2000. Fluidized bed combustion of Australian bagasse. Fuel 79, 123–130.

Rasul, M.G., Rudolph, V., Čársky, M., 1999. Segregation potential in binary gas fluidized beds. Powder Technology 103, 175–181.

Rowe, P.N., Nienow, A.W., 1976. Particle Mixing and Segregation in Gas Fluidised Beds. A Review. Powder Technology 15, 141–147.

Rowe, P.N., Nienow, A.W., Agbim, A.J., 1972. The Mechanisms by which Particles Segregate in Gas Fluidised Beds - Binary Systems of Near-Spherical particles. Transactions of the Institution of Chemical Engineers 50, 310–323.

Sarkar, S., Van der Hoef, M.A., Kuipers, J.A.M., 2009. Fluid–particle interaction from lattice Boltzmann simulations for flow through polydisperse random arrays of spheres. Chemical Engineering Science 64, 2683–2691.

Tanaka, Z., Song, X., 1996. Continuous separation of particles by fluidized beds. Advanced Powder Technology 7, 29–40.

Van der Hoef, M.A., Beetstra, R., Kuipers, J.A.M., 2005. Lattice-Boltzmann simulations of low-Reynolds-number flow past mono- and bidisperse arrays of spheres: results for the permeability and drag force. Journal of Fluid Mechanics 528, 233–254.

Wu, S.Y., Baeyens, J., 1998. Segregation by size difference in gas fluidized beds. Powder Technology 98, 139–150.

Yin, X., Sundaresan, S., 2009. Fluid-particle drag in low-Reynolds-number polydisperse gas-solid suspensions. AIChE Journal 55, 1352–1368.

Zhou, Z.Y., Yu, A.B., 2009. Simulation of the Flow and Segregation of Particle Mixtures in Liquid Fluidization, in: Powders and Grains. AIP Conference Proceedings 1145, pp. 1–4.

Čársky, M., Pata, J., Veselý, V., Hartman, M., 1987. Binary system fluidized bed equilibrium. Powder Technology 51, 237–242.

Figure Captions

Figure 1. Sketch of the evolution towards possible fluidization and segregation scenarios for initially mixed LB-HS binary beds.

Figure 2. Dependence of the pure drag force ratio (a) and net drag force ratio (b) on the size ratio. The pure drag force ratio plot is unique, while the net drag force ratio depends moderately on composition and voidage (values in the legend).

Figure 3. Segregation direction map with equilibrium lines at voidage $\varepsilon = 0.4$. Part (a) shows the map in terms of species property ratios (Eq. 27) at different compositions; in part (b) the equilibrium line is plotted in terms of the average properties and those of species 2 (Eq. 24). In the sketches, arrows next to each particle type represent the segregation direction.

Figure 4. Segregation direction equilibria and equal minimum fluidization velocity curves for viscous (a) and inertial flows (b). Segregation/fluidization combinations give rise to behaviors as diagrammatically shown by sketches A, B and C and the corresponding zones in the map.

Figure 5. Sequence of photographs showing three different time instants during the fluidization of a mixture of 570 μm diameter glass ballotini (ρ = 2480 kg/m^3) and 229 μm diameter steel shots (ρ = 7600 kg/m^3). The lower, bubbling layer is nearly pure in steel shots and the upper, static layer is a glass-rich mixture.

Figure 6. Comparison of model predictions and experimental observations for the segregation direction in the examined systems (see Table 5). Each experimental datum is shown with a symbol corresponding to the flotsam component (small solid symbols for the HS species and big open symbols for the LB species) in segregated systems or crosses for systems reported as mixed. Model predictions are discriminated by the curve, as shown in Fig. 3b, i.e. the HS (LB) species acts as flotsam above (below) the curve.

Figure 7. Analysis of the systems exhibiting a change of segregation direction in experiments and comparison with the predicted change upon crossing the theoretical equilibrium line. Data from Naimer et al. (1982) and Joseph et al. (2007) (a), Formisani et al. (2008a) (b), Chiba et al. (1980) (c) and this work (d).

Extension and validation of the Particle Segregation Model for bubbling gas-fluidized beds of binary mixtures

Francesco P. Di Maio, Alberto Di Renzo*, Vincenzino Vivacqua

Department of Environmental and Chemical Engineering, University of Calabria
Via P. Bucci, Cubo 44A, 87036 Rende (CS), Italy

** Corresponding author (A. Di Renzo): T.: +39 0984 496654, F.: +39 0984 496655; Email: alberto.direnzo@unical.it*

Abstract

The present work elaborates on the Particle Segregation Model (PSM) recently developed (Di Maio, F.P., Di Renzo, A., Vivacqua, V., 2012. Powder Technology 226, 180–188) to address the prediction of the "segregation direction" in fluidized beds, i.e. the flotsam/jetsam behavior of the solid components in the bubbling bed. In the original derivation, the PSM was obtained in the limit of viscous flow, i.e. for particle Reynolds' number up to 5. In the present contribution we prove that its formulation is more general, and that it can be extended without modifications to any flow regime. Starting from the force balance on one particle, the competition of mechanisms in mixtures whose components' size difference effect counteracts that of density difference is contemplated. The macroscopic result is expressed, analytically and without adjustable parameters, in terms of the size ratio, density ratio, voidage and bed composition. The knowledge of the segregation direction can be combined with a comparison of the pure components' minimum fluidization velocities yielding, although only under the complete segregation hypothesis, a prediction of the different segregation/fluidization patterns. Extensive model validation is carried out by: (i) comparison of the predicted segregation direction against many experimental observations reported in the literature (53 systems) and with tests (7 systems) carried out in the present work; (ii) visualization in a 2D rig of segregated beds predicted to exhibit a layer fluidized *below* the stagnant rest of the material; (iii) observation of float/sink behavior of few large spheres immersed in the bubbling bed. Agreement for nearly all the considered systems is found, with remarkable segregation reversal predictions with bed composition for three of them.

Keywords: Fluidization; Mixing; Multiphase flow; Particulate Processes; Drag force; Segregation.

1. Introduction

Fluidized beds composed of more than one solid component are often encountered in industrial processing of granular materials. In many cases, the complex two-phase hydrodynamics of the bubbling regime leads to unpredictable segregation behavior that, in turns, severely affects the performance of key fluidization-based process units such as reactors, combustors, gasifiers, incinerators. As a consequence, their design is still dominated by empiricism. This is particularly true for charges involving irregular solids like most biomasses or municipal solid wastes (Cui and Grace, 2007). In other cases, the very aim of the unit is to drive the separation of two or more granular materials, like in mineral dressing and solids classification (Tanaka and Song, 1996; Olivieri et al., 2009).

In a bubbling gas fluidized bed, agitation due to bubbles is usually deemed responsible for the homogeneity of properties in the emulsion like temperature and gas-phase species concentration in the bed. However, if dissimilar solids are simultaneously utilized, their different fluidization behavior may lead to inhomogeneous solid composition along bed height, with the one component accumulated at the top usually referred to as *flotsam* and the other one as *jetsam* (Rowe et al., 1972). In some cases, segregation may prevail, typically at the lower velocities, with the suspended bed appearing as a superposition of two distinct bubbling layers. When the differences in properties are even more extreme, elutriation of one solid occurs before the full bed reaches suspension by the gas, rendering the fluidization of the whole mixture practically impossible. Generally, a gradually changing component distribution along bed height is observed.

Component properties in a fluidized mixture can also change as a result of the evolution of the chemical/physical process in the unit, leading to a progressive shift of a component location inside the bed and, possibly, local defluidization, with significant impact on the process performance (Ekinci et al., 1990).

Various papers in the literature report attempts at a characterization of the mixing and segregation patterns of binary mixture in bubbling gas-fluidized beds. Historically, significant progress in understanding multicomponent fluidization started in the seventies (Rowe et al., 1972; Rowe and Nienow, 1976; Nienow et al., 1978; Chiba et al., 1979). Numerous experimental works have since focused on the individual effect of size segregation and density segregation, or a combination of both (see e.g. Beeckmans and Stahl, 1987; Čársky et al., 1987; Hoffmann et al., 1993; Wu and Baeyens, 1998; Rasul et al., 1999; Rasul and Rudolph, 2000; Marzocchella et al., 2000; Formisani et al., 2001, 2008a; Gilbertson and Eames, 2001; Olivieri et al., 2004; Dahl and Hrenya, 2005;

Joseph et al., 2007; Jang et al., 2010). More recently, computational simulations have supplemented these investigations. Different research groups have utilized simulation approaches based on a two-fluid model (TFM) representation (Huilin et al., 2003; Gera et al., 2004; Qiaoqun et al., 2005; Owoyemi et al., 2007; Mazzei et al., 2010; Chao et al., 2012) or a combination of computational fluid dynamics and the discrete element method (DEM-CFD) (Hoomans et al., 2000; Bokkers et al., 2004; Feng et al., 2004; Feng and Yu, 2007; Di Renzo et al., 2008) to examine the phenomenon in more detail.

Attempts have been made at classifying and predicting the behaviors of binary mixture in gas-fluidized beds in terms of the particle properties and bed conditions. The first comprehensive 1-D differential model for segregation was proposed by Gibilaro and Rowe (1974). It is worth mentioning that later works showed that the evaluation of parameters in the general case is rather complicated (see e.g. Naimer et al., 1982). Among the studies devoted to the classification, the first simple and objective criterion to distinguish between the various categories was proposed by Chiba et al. (1980). Based on the analysis of the concentration profile of various solid pairs, they proposed conditions expressed in terms of combinations of size, density and minimum fluidization velocity of the two solids. An empirical criterion of mixability or non-mixability in fluidized beds was proposed by Tanaka et al. (1996), in which density and size ratios where combined with minimum fluidization voidage. Based on a relatively small amount of data, a line separating mixing and segregating beds was also proposed by Rasul et al. (1999). Recently, Rao et al. (2011) reviewed a significant number of data from the literature and carried out a few specific experiments to classify fluidized mixtures according to their observed behavior. All of these works are based primarily on the observations of real or simulated experiments, whilst a theoretical framework for a comprehensive understanding of the degree of mixing or segregation still lacks.

The full prediction of the concentration profile along bed height in the general case is a very complicated task. However, excluding trivial cases, even the question of which species in a segregating binary bed does play the role of flotsam, as opposed to jetsam, is essentially still open. It is well documented that a small size or density characterize solids that tend to float while larger or denser solids are typically found to sink to the bottom of the bed. When the two properties act in contrasting directions, the determination of the role of the two components (i.e. flotsam and jetsam) is far less trivial. It is convenient to start by considering an initially mixed bed and attempt to predict the possible segregation "direction" of the two species. Following the terminology introduced by Rowe and Nienow (1976), H and L will be used to denote higher and lower densities, respectively, and B and S to denote larger and smaller particle sizes, respectively. Thus, the focus

here will be on LB-HS mixtures. Traditionally, the difficulties arise because the mechanical equilibrium equations applied to the whole bed or to slices of the bed do not help, since in a fluidized bed the weight of every part of the system is balanced by the hydrodynamic action of the up-flowing fluid. Therefore, no information on the relative movement of the solids can be extracted and all segregation possibilities are admitted.

Additional complications arise when considering fluidization scenarios as they result from segregation patterns. Phenomenologically, segregation is stronger if higher velocities are avoided, as vigorous bubbling tends to favor bed mixing. On the other extreme, full bed suspension and particle mobility is a necessary requirement; otherwise, solids rheology may prevent the establishment of pure drag vs. gravity balance, additionally rendering the result dependent upon the initial pouring procedure. As a consequence, in focusing on the segregation tendency of a homogeneously mixed system, low velocities, slightly above the value required for bed suspension, should be most appropriate for our purposes. As particles' mobility allows segregation to take place, flotsam particles will be pushed upwards and jetsam particles will sink to the bottom of the bed. However, the flotsam is not necessarily the fluidized species, as there is no relation linking the tendency to segregate up or down *in the mixture* with the minimum fluidization velocity of the *pure* components. Therefore, four possible (simplified) segregation/fluidization scenarios can, in principle, be attained, as schematically depicted in Figure 1. In type A (Fig. 1a), the LB species is pushed to the surface (acting as flotsam), undergoing regular fluidization on top of the other component; in type B (Fig. 1b) the HS component segregates to the bottom of the bed, being fluidized as jetsam *below* the packed LB species; in type C (Fig. 1c) the HS component will float to the surface and get fluidized; in type D (Fig. 1d) the LB species will tend to act as jetsam and be fluidized below the packed bed of the other solid. However, not all cases are necessary plausible. Type A is certainly the most common condition observed, with the denser component packed at the bottom and the less dense species fully fluidized on top of it. Also, evidences of type-C segregation have been reported by Chiba et al. (1980). On the contrary, types B and D appear, at first, rather unexpected.

The present paper is aimed primarily at addressing the issue of the segregation direction in general and theoretically sound terms. The characterization of the segregation behavior of such systems will be proposed by working out a generalization of the Particle Segregation Model (PSM), as introduced by Di Maio et al. (2012). Previously, the model was restricted to low-Reynolds number flows, as it resulted from two conditions assumed: Carman-Kozeny relationship was utilized to express the drag force in monodisperse systems and van der Hoef et al. (2005) approach, derived in

the viscous-flow limit, was adopted to formulate the force in bi-disperse systems. It will be shown here that both origins of the limitation can be removed without amendments to the PSM formulation. In relation to the fluidization patterns developing as a result of the segregation (Fig. 1), an attempt will be made to model the observable fluidization/segregation scenarios as a function of the relevant system properties.

In Section 2 a derivation of the drag force for bi-disperse systems, required for the Particle Segregation Model, is presented in more general terms than previously (Di Maio et al., 2012). Section 3 presents the generalization of the PSM formulation for any flow regimes. In Section 4 the implications of the PSM predictions are discussed. Materials and methods adopted in the experiments are described in Section 5 and all validation steps are presented in Section 6.

2. Hydrodynamic force on a particle immersed in a bi-disperse suspension

In the Particle Segregation Model the segregation direction results from a balance of the hydrodynamic force and gravity on a single particle in the mixture. The critical element in the balance is the drag force exerted by the fluid in a bi-disperse suspension (Di Maio et al., 2012). The formulation of accurate and generally valid expressions for the local fluid-particle interaction has always stimulated research efforts. In particular, account for the effects of polydispersity of the suspension on the drag force acting upon a specific particle is receiving special attention. Various expressions for such force have been proposed (Van der Hoef et al., 2005; Holloway et al., 2009; Yin and Sundaresan, 2009; Cello et al., 2010) and simulations seem to confirm their validity (Beetstra et al., 2007; Di Renzo et al., 2011). Here, we propose a formulation that overcomes the limitations of viscous-flow conditions with respect to previous attempts (Di Maio et al., 2012; Di Renzo et al., 2012).

The total interaction force N experienced by a particle of a bed is typically subdivided for convenience into a pressure gradient term and a *pure* drag force F:

$$N = V\left(-\frac{dp}{dz}\right) + F \tag{1}$$

in which V is the particle volume, p is the fluid *net* pressure (i.e. free from the hydrostatic contribution, see e.g. Cello et al., 2010), and z is the vertical coordinate.

Consider a uniform mixture of kt monodisperse solids species, namely the bed components. Under fully-developed, steady-state flow conditions, the relation between the overall pressure drop across

the bed and the drag force on individual particles can be expressed as the sum of each component's weighted contribution (Cello et al., 2010), i.e.:

$$-\frac{dp}{dz} = \frac{6(1-\varepsilon)}{\pi} \sum_{k=1}^{kt} \frac{x_k N_k}{D_k^3} \tag{2}$$

where x_k is the volumetric fraction of the species k and ε is bed voidage. In analogy with the monodisperse case, the overall pressure drop across the bed can be referred to an average particle-scale force, to be calculated at an appropriate average diameter, i.e.:

$$-\frac{dp}{dz} = \frac{6(1-\varepsilon)}{\pi} \frac{\overline{N}}{\overline{D}^3} \tag{3}$$

This simply corresponds to introducing the two average variables, and it is always possible to find a suitable definition of one quantity, typically the diameter, and derive the definition of the other one.

As a convenient measure of the size dispersion in relation to species i, the polydispersion index proposed by van der Hoef et al. (2005) is recalled:

$$y_i = \frac{D_i}{\overline{D}} \tag{4}$$

It is now postulated that the force experienced by a particle in the mixture can be expressed in terms of the average force:

$$N_k = \alpha_k \overline{N} \tag{5}$$

i.e. by introducing the dimensionless force specification coefficients α_k.

By substituting Eq. (5) into Eq. (2) and equating the overall pressure drop to Eq. (3), one obtains a constraint on the definitions involved to guarantee model consistency, i.e.:

$$\sum_{k=1}^{kt} \frac{x_k \alpha_k}{y_k^3} = 1 \tag{6}$$

Note that by setting $\alpha_k = y_k^3$ Eq. (6) is trivially fulfilled. Other possible expressions for α_k are related to the definition of the average diameter $\overline{D}$ and can include the polydispersion index y as well as the voidage.

An appropriate average diameter is Sauter's definition (Gibilaro et al., 1986):

$$\overline{D} = \left(\sum \frac{x_k}{D_k} \right)^{-1} \tag{7}$$

This leads to another possibility for the specification coefficient, named $\alpha_k = y_k^2$. Furthermore, any linear combination of the kind:

$$\alpha_k = a y_k^2 + (1-a) y_k^3 \tag{8}$$

where *a* is a coefficient to be defined, is in fact consistent with Eq. (6).

Similar considerations and derivations apply if the problem is formulated in terms of pure drag force *F* instead of *N*. Specification coefficients are introduced as:

$$F_k = \beta_k \overline{F} \tag{9}$$

with the requirement that $\overline{F} = \varepsilon \overline{N}$ and

$$\sum_{k=1}^{kt} \frac{x_k \beta_k}{y_k^3} = 1 \tag{10}$$

so that a plausible expression for β_k is

$$\beta_k = b y_k^2 + (1-b) y_k^3 \tag{11}$$

where *b* is another coefficient to be defined.

A direct comparison of the expressions for F_k and N_k leads to the following two relations, one between the two forces:

$$F_k = \varepsilon \frac{\beta_k}{\alpha_k} N_k \tag{12}$$

and one between the specification coefficients:

$$\alpha_k = \beta_k \varepsilon + (1-\varepsilon) y_k^3 \tag{13}$$

Amongst the many possibilities, three examples of compatible formulations of the specification coefficients are listed in Table 1.

In order to discriminate between the possibilities, considerations on an extreme case appear useful. Let us analyse the force experience by a single, very large particle immersed in a fluidized bed of

fine material. Let us denote bed material with index 1 and the particle with index 2. It is known and well documented that the particle will be in equilibrium when its density ρ_2 equals the bulk density of the suspended bed $\rho_1(1-\varepsilon)$ (see e.g. Kunii and Levenspiel, 1991). The above concept can be cast in form of a balance of the net force acting on the sphere and its weight:

$$\alpha_2 \overline{N} = \rho_2 \frac{\pi D_2^3}{6} g \tag{14}$$

whence we shall derive the density ρ_2 of the sphere that is in equilibrium with the fluidized bed. If the particle is just one and very large we have that $D_1/D_2 \to 0$, $x_1 \to 1$, $\overline{D} \to D_1$ and $y_2 \to D_2/D_1$. In the bed the average net force assumes the value necessary to support the weight of a fine particle. Thus, invoking also the coefficient *a*, we get:

$$\left[a\left(\frac{D_2}{D_1}\right)^2 + (1-a)\left(\frac{D_2}{D_1}\right)^3 \right] \rho_1 \frac{\pi D_1^3}{6} g = \rho_2 \frac{\pi D_2^3}{6} g \tag{15}$$

whence, after simple manipulations and using the vanishing size ratio:

$$\rho_2 = \rho_1(1-a) \tag{16}$$

The obvious correct choice is then $a = \varepsilon$, corresponding to case 1 in Table 1, leading to:

$$\varepsilon y_k^2 + (1-\varepsilon) y_k^3 \tag{17}$$

The definition of the specification coefficients allows calculating the ratio of drag forces for the two particle species. Owing to the fact that such ratio is in fact the ratio of the specification coefficients, its dependence on the size ratio and other variables is different depending on the drag force considered. Fig. 2 shows the plots of the pure and net drag forces versus the size ratio. While the pure drag force ratio scales only with the square of the size ratio (Fig. 2a), that of the net forces exhibits a dependence, though very limited, on composition – through the average diameter – and voidage (Fig. 2b). All net force ratio curves in Fig. 2b lay between the quadratic and cubic dependence on size ratio. The results demonstrate that the two forces, both sometimes equivocally called "drag force", are indeed conceptually different. Analyses of the effect of using different drag laws for binary mixtures (like in e.g. Okayama et al., 2006; Zhou and Yu, 2009) require special care to avoid any possible confusion.

The reader will note that the result found for α_k in Eq. (17) (Case 1 in Table 1) corresponds to the expression derived, under the assumption of viscous flow, by van der Hoef et al. (2005). The

difference is that in the present derivation no specific flow regime was required. The agreement in validation tests for slight modifications of the above-mentioned model in random bidisperse arrays computed by lattice-Boltzmann simulations (Van der Hoef et al., 2005; Sarkar et al., 2009) and for the layer inversion phenomenon in liquid-fluidized beds by DEM-CFD simulations (Di Renzo et al., 2011) provides an indirect confirmation of the sound physical basis of the approach. However, further elaborations by comparison of results at the macroscopic scale with experimental results are required, some of which are discussed below.

3. Generalization of the particle segregation model (PSM)

The particle segregation model (PSM) is based on the balance of the gravitational and hydrodynamic forces acting on a single particle immersed in a fluidized bed of two solids. In our previous work (Di Maio et al., 2012), the model was described for the case of a single particle immersed in a bed of a different fluidized suspension and for binary mixtures. However, discussion was limited to the viscous flow regime. After a summary of the model foundations, we will show that the general specification coefficients described in Section 2 along with expressions for the average drag force valid for any flow regime allow overcoming the limitation to low-Reynolds' number flows.

In the case of a gas-fluidized binary mixture composed of species 1 and species 2, we propose to set the force balance on one particle of species 2, by convention the bigger particle. Model assumptions are as follows:

a. bed is composed of two fully mixed spherical solids;

b. binary bed is in the fluidized state, i.e. the total sum of the hydrodynamic forces exerted by the fluid equals the total bed weight;

c. voidage is uniform.

The model is based on a rather elementary concept (Di Maio et al., 2012), named that each particle in the bed is subjected to the action of gravity and momentum transfer by the fluid, which may be unbalanced. Indeed, it should be noted that assumption (b) apply to the bed as a whole and it does not imply that *each* particle, taken individually, is at equilibrium with respect to drag and gravity. It is fully compliant with the hypotheses that the particles belonging to one species exhibit domination of drag over gravity and the reverse occurs for particles belonging to the other species. Therefore, eventually the force balance on the test particle would indicate whether it, and all particles of the

same species, will be pushed upwards by the action of the fluid or will tend to sink to the bottom as a result of the dominance of weight.

Because of assumption (b) the pressure gradient developing across the bed can be expressed in terms of the bulk density of the binary suspension as:

$$-\frac{dp}{dz} = \bar{\rho}(1-\varepsilon)g \tag{18}$$

where

$$\bar{\rho} = \rho_1 x_1 + \rho_2(1-x_1) \tag{19}$$

As far as the drag force is concerned, it is necessary to apply Eq. (9) at the velocity necessary to suspend the emulsion phase of the (mixed) binary bed, i.e. the minimum fluidization velocity $\bar{u}_{mf}$ of an equivalent solid of density $\bar{\rho}$ and diameter $\bar{D}$. In our previous derivation (Di Maio et al., 2012), the hypothesis of viscous flow led to the following formula for the pure drag force on the particle of species 2 at the relevant velocity:

$$F_2\big|_{u=\bar{u}_{mf}} = \frac{1}{6}\pi g \varepsilon \bar{\rho} \bar{D} D_2^2 \tag{20}$$

However, it is straightforward to show that the above relation holds for any given dependence of the force on the velocity, e.g. using expressions derived from Ergun's pressure drop (Ergun, 1952) or Di Felice's formula (Di Felice, 1994). In fact, making use of the equivalence between the net drag force and weight of the average species, evaluation of the above force in more general terms is obtained by:

$$F_2\big|_{u=\bar{u}_{mf}} = y_2^2 \bar{F}\big|_{u=\bar{u}_{mf}} = y_2^2 \varepsilon \bar{N}\big|_{u=\bar{u}_{mf}} = y_2^2 \varepsilon \bar{\rho} \frac{\pi \bar{D}^3}{6} g = \frac{1}{6}\pi g \varepsilon \bar{\rho} \bar{D} D_2^2 \tag{21}$$

without the assumption of a particular flow regime or drag expression.

The condition for the test particle to be pushed upwards arises from the comparison of the net fluid-particle force, as evaluated in Eq. (1), at the minimum fluidization velocity of the mixture and the particle's weight, as follows:

$$V_2 \bar{\rho}(1-\varepsilon)g + \tfrac{1}{6}\pi g \varepsilon \bar{\rho} \bar{D} D_2^2 > V_2 \rho_2 g \tag{22}$$

By introducing the following density and size ratios:

$$\bar{s} = \frac{\rho_2}{\bar{\rho}} \tag{23a}$$

$$\bar{d} = \frac{\bar{D}}{D_2} \tag{23b}$$

Eq. (22) reduces simply to

$$\bar{s} < 1 - \varepsilon + \varepsilon \bar{d} \tag{24}$$

It is convenient to express the above ratios also in terms of the corresponding species properties, giving:

$$\bar{s} = \left(\frac{x_1}{s} + 1 - x_1 \right)^{-1} \tag{25a}$$

$$\bar{d} = \left(\frac{x_1}{d} + 1 - x_1 \right)^{-1} \tag{25b}$$

where

$$s = \frac{\rho_2}{\rho_1} \tag{26a}$$

$$d = \frac{D_1}{D_2} \tag{26b}$$

Eq. (24) can include the equilibrium dictated by the equality and be expressed in terms of *s* and *d*, yielding:

$$s \leq \frac{(1-\varepsilon)(1-d)x_1 + d}{(1-x_1)(d+\varepsilon-\varepsilon d) + x_1} \tag{27}$$

Summarizing the above derivation, we have that given solids properties and bed composition Eq. (27) allows predicting whether species 2 will tend to be pushed upwards, i.e. act as flotsam (if the inequality is satisfied), or settle to the bottom, representing the jetsam in the mixture (if the opposite inequality applies).

It shall be remarked that only the initial tendency is currently predictable through the PSM, while no information is provided on the extent of the segregation at the end of the process, i.e. its steady-state "intensity".

3.1 Individual minimum fluidization velocities

It is interesting to try to relate the results expressed by Eq. (27) and the minimum fluidization velocities of the individual bed components. In fact, in the past their values determined the role of *fluidized* and *packed* attribute to the mixture components (Chiba et al., 1980).

Let us focus on the simplified condition of complete segregation of the two components, a system where the individual u_{mf} represent directly the relevant velocities, i.e. there is no interaction of the two solids on their fluidization behavior. Under this circumstance, the two solids may be regarded simply as two monocomponent beds one on top of the other.

Indications on the suspended component in the bed will therefore be obtained by comparing the two minimum fluidization velocities. Assuming uniform voidage and the same flow regime throughout the bed, the conditions for the two solids to have the same minimum fluidization velocity can be expressed by:

$$\rho_1 D_1^2 = \rho_2 D_2^2 \qquad \text{(viscous regime)} \qquad (28)$$

$$\rho_1 D_1 = \rho_2 D_2 \qquad \text{(inertial regime)} \qquad (29)$$

which, in terms of the dimensionless variables introduced, become:

$$s = d^2 \qquad \text{(viscous regime)} \qquad (30)$$

$$s = d \qquad \text{(inertial regime)} \qquad (31)$$

By comparing Eqs. (30-31) and Eq. (27) we found that the condition of equal u_{mf} of the pure components does not correspond to the equilibrium of forces when the two solids are mixed. The two results appear rather independent and can therefore be used distinctly for the segregation, the former, and the fluidization, the latter, respectively.

4. Model predictions

4.1 Segregation direction from the PSM

The condition prescribed by Eq. (27) relating the density and size ratios, voidage and composition is the main result of the Particle Segregation Model and is shown here to be independent of the flow regime. Equilibrium conditions result as shown, in terms of components' density and size ratio from Eq. 27, in Fig. 3a and, in terms of component-to-average density and size ratio from Eq. 24, in Fig. 3b. Note that explicit dependence of the bed composition appears in Fig. 3a, while a unique master

curve is obtained, for a given voidage, when the ratios involve the average properties, Fig. 3b. It is the case to mention that the influence of voidage values is relatively modest, as changes within the range of interest for mixtures (e.g. between say 0.3 and 0.4) cause only slight displacements of the curves in the plots of Fig. 3, as it can be easily verified using Eqs. (24) or (27).

Considerations on the inequality allow identifying characteristic segregation patterns. Fig. 3 shows how the chart is subdivided into a lower zone, in which the bed tend to segregate with the LB component acting as flotsam, and an upper zone, in which the role of flotsam is played by the HS component. When using Fig. 3a, the reader will notice that the limit curve discriminating zones with different segregation direction is the one corresponding to the overall volume composition x_1 in the bed.

4.2 Segregation/fluidization patterns

A plot of the results of Eq. (30) and (31) on the *s*-*d* diagram allows completing the characterization of the expectable scenarios, as predicted by the combination of the PSM and the comparison of the pure components' minimum fluidization velocities in the complete segregation case (Fig. 4). Diagrams showing the viscous and inertial regime cases are shown in Figs. 4a and 4b, respectively. Note that a distinct plot is necessary for the two flow regimes only because of the difference in the equal minimum fluidization conditions.

For property ratios belonging to the lower part of the plot (zone A in Fig. 4) the systems is predicted to evolve by segregating the less dense component towards the top of the bed, which consequently undergoes free fluidization on top of the rest of the bed.

Under combinations of densities and sizes belonging to the middle zone of Fig. 4 (zone B), i.e. above the equal u_{mf} curve and below the equilibrium line at the given system composition, the initially mixed system evolves in the same segregation direction as the previous case. However, in this case the segregated component that would be (if pure) over-fluidized is the HS species, which tends to settle to the bottom of the bed. Therefore, this would be fluidized below the stagnant rest of the bed.

If the density ratio is not very different from unity and size difference is sufficiently large (zone C in Fig. 4), a binary mixture is predicted to tend to segregate with the denser component (fluidized) at the top of the bed. Thus, above equilibrium lines the denser component tends to act as flotsam in the mixture. In this case, the system exhibits fluidization of the HS species on top of the rest of the bed.

In summary, the combination of the results of the particle segregation model, Eq. (27), and the equal minimum fluidization condition, Eq. (30) or (31), establish the basis for a theoretically sound framework for the characterization of the segregation tendency of complex mixtures. As introduced elsewhere (Di Maio et al., 2012) and extended below, experimental findings appeared in the literature do not contradict the picture described above.

5. Experimental method

Specific experiments have been carried out in an attempt to focus the attention on the behavior of material pairs endowed with properties falling in particular areas of the *s*-*d* plane. All other experimental data were collected from tests in a 10-cm ID transparent cylindrical fluidization column, equipped with a 4-mm-thick plastic porous distributor. The experimental procedure is as follows. Starting from a well-mixed packed bed, whose homogeneity has been ensured by slowly pouring several mechanically pre-mixed portions of the total solid mass (Formisani et al., 2011), the fluidizing air flow was increased up to a velocity value slightly above the minimum fluidization velocity of the mixture. In order to obtain data relevant to the concentration profile along the column, the "freezing" procedure was applied, as documented by various authors (Rowe and Nienow, 1976; Nienow et al., 1978; Chiba et al., 1979, 1980; Beeckmans and Stahl, 1987; Čársky et al., 1987; Hoffmann et al., 1993; Wu and Baeyens, 1998; Formisani et al., 2001, 2008a, 2008b). To this regard a valve on the feed line was employed to suddenly cut the air flow off; afterwards, horizontal layers of particles were drawn from the top of the column, separated by sieving and weighted. The concentration profile was used to determine univocally the segregation direction.

In addition to tests in the cylindrical set-up, qualitative observations have been conducted visually in a 2D transparent fluidization set-up (15 cm by 1.5 cm cross-sectional area and porous-plate distributor), whose results are reported and discussed in Section 6.1.

Measurements involved four types of closely sieved, nearly spherical solids: glass ballotini (GB), molecular sieves (MS), steel shots (SS), bronze shots (BS) and zirconium silicate spheres (ZS). Their properties are listed in Table 2. From these cuts, the four mixtures listed in Table 3 have been prepared. In all experiments, the component masses were adjusted so to ensure a packed bed aspect ratio initially set equal to 1.7.

The segregating behavior of three GB-MS mixtures has been experimentally investigated at various size ratios, keeping the component volume fraction $x_1 = 0.5$. The effect of composition has been addressed for the GB162-MS824 bed. The choice of the mixture BS70-SS229 has been aimed at

producing data in a region of the *s*-*d* plane where the availability of experiments in the literature is scarce. Finally, an additional binary bed was examined, ZS168-GB898, whose component size ratio is similar to another GB-MS system.

6. Comparison of predictions and measurements

6.1 Observation of type B segregation patterns

Of the four extreme segregation types discussed in Section 1, type A is the most commonly encountered one. As already mentioned, behavior ascribable to type C was also previously reported and classified, mostly as an exception. Fluidization below a packed bed, such as typical of cases B and D, is much more difficult to conceive. In an attempt to observe type B segregation, a mixture of bigger glass ballotini (D = 570 μm) and smaller steel shots (D = 229 μm), initially mixed, was fluidized in the 2D rig to highlight the presence of a top- or bottom-localized bubbling. With reference to Fig. 4a, the mixture (d = 0.40 and s = 0.33) falls inside the zone whose corresponding extreme segregation pattern is type B. Visual observation of the fluidization process, in fact, confirmed the presence of a bed composed of a lower bubbling layer and an upper packed layer (Fig. 5). In Fig. 5a-5c a sequence of three photographs of the observed behavior are reported. The mixture did not segregate completely, but a clear interface where bubbles ended up "absorbed" was distinctly visible. With respect to the pre-fluidization stage, the system appeared segregated, though not completely, and fully at suspension, i.e. with the gas pressure drop balancing the bed weight. In order to allow for the formation and growth of bubbles the initial mixture lifted slightly, while at the same time material from the bottom of the bed fell, undergoing fluidization and separation. However, since this transient detachment did not involve the entire mass up to the surface, the upper portion of the bed eventually remained supported by the bubbling bed. As a final note, it is remarked that the process resulted fully stable, in the sense that no further evolution was observed after hours of operation under the conditions shown in Fig. 5. Repeated trials in the same apparatus and experiments in the 3D column showed no qualitative differences. It is the case to mention that the presented observations are also in line with those reported by Formisani et al. (Formisani et al., 2012), who denoted such behavior as *bottom fluidization* vs. the most common *top fluidization*.

Conditions with the LB solid fluidizing below a packed bed composed mostly of the HS species, i.e. type D segregation, as hypothesized in Section 1 (Fig. 1d), was neither predicted by the model nor observed in any experiments, and can likely be considered as not plausible.

6.2 Very large particles in a fluidized bed

A first way to examine the predicting capabilities of the PSM is to compare the segregation direction with the experimentally observed prevalence of individual spheres in the upper region or in the lower region of a fluidized bed of fine particles. A useful experimental analysis of this kind was conducted by Oshitani et al. (2004). They investigated the tendency of a relatively small amount of large particles of relatively low density to appear towards the surface or the bottom of a vibro-fluidized bed of fine (and denser) glass ballotini. Data extracted from the work along with the corresponding model predictions are reported in Table 4. In the experiments 6-Nylon spheres tend to float over the bed for the entire range of sphere diameters investigated, while the Teflon sphere tends to sink for all sizes of the bed particles. Model predictions agree in all reported cases, demonstrating the capability to discriminate even between two systems relatively similar in *s* and *d* ratios but exhibiting a different segregation direction, named System 1 and System 6 in Table 4.

6.3 Segregation direction in binary fluidized beds

A review of the experimental findings available in the literature on gas-fluidized binary beds with the sought properties revealed a significant number of works, although often with a variable extent of the details reported. Most of the systems were present already in our previous comparisons (Di Maio et al., 2012; Di Renzo et al., 2012), except the ones characterized by higher particle Reynolds number. The properties of all the collected systems (53 systems from 15 different references) are listed in Table 5, together with the 7 systems investigated in the present work and detailed in Section 5. Note that the vast majority of them exhibit the LB solid as flotsam, some of them are characterized by a change of the flotsam component with bed composition and few systems appear with the HS species acting as flotsam. Table 5 also contains the predictions of the PSM as regards the segregation direction, with specific computation for different compositions whenever the experimental datum was not available.

All systems are plotted in Fig. 6 along with the equilibrium curve prescribed by the PSM. Note that each point represents values of $\bar{s}$ and $\bar{d}$, as determined by the size and density ratios of the solids, namely *s* and *d*, and bed composition (Eq. 26). In the plot, the behavior exhibited is represented using different symbols depending upon the type of segregating system observed: big open symbols are used to denote conditions where the LB species is flotsam, small solid circles when the HS species is flotsam and crosses when the system is reported as mixed. The straight line denotes the equilibrium of the tendencies as prescribed by the PSM (Eq. 24), so it discriminates between the two segregation directions. Fig. 6 and Table 5 show that the separation of behavior predicted by the

PSM corresponds to the experimental observations for a very broad range of different solids combinations and operating conditions. Exceptions to the proposed rule occur in few cases where the separation direction component is reversed with respect to the predictions and in those cases where bed mixing is observed. As reported in Table 5, for some binary mixtures data are available at different bed compositions, of particular importance being those where a corresponding change of behavior is observed. In order to examine the effect of a change of composition in Fig. 6 for a given solid pair, it is useful to note that average ratios $\bar{s}$ and $\bar{d}$ change according to Eqs. 25a-b. In particular, they both tend to unity as x_1 tends to zero and they tend to the corresponding values s and d as x_1 tends to one. Therefore, the location of the point moves as bed composition varies. Now, if the model predictions are correct, then curves corresponding to binaries segregating always in the same direction should be located entirely on one side of the equilibrium line, while those representing pairs exhibiting a reversal should cross the PSM line. Fig 7 shows such curves along with symbols, using the same convention as in Fig. 6, corresponding to experimental measurements for selected systems. Fig. 7a shows the comparison of predictions and observations in cases of constant segregation direction (LB is flotsam), while Figs. 7b-d show three cases in which a change of behavior is observed. For the system examined by Formisani et al. (2008a) (Fig. 7b), the unusual behavior (HS species as flotsam) is reported at lower values of x_1 while the bed tends to mix at higher concentrations. The model also predicts a change of behavior with composition, although a sharper one directly to the opposite segregation direction, for a composition compatible with the experiments. For the system reported in Chiba et al. (1980), the curve representing different compositions of the examined solids pair is also shown to cross the equilibrium curve (Fig. 7c). However, the predicted composition corresponding to the change of the direction results higher than the experimentally observed value. The third mixture, examined in the present work, exhibits a change of segregation pattern at the cross with the equilibrium line (Fig. 7d). In the experiments, the segregation intensity observed in both directions appeared modest and the bed could have also been judged essentially mixed at all compositions, with a slight tendency of either species to float to the surface in the two more "extreme" compositions.

It is worth noting that, despite the relatively coarse approximations of the model, the simplicity of the obtained relations and the lack of adjustable parameters, in all cases where segregation inversion or, at least a change of behavior, was observed in experiments, the corresponding curves cross the model line on the $\bar{s}$-$\bar{d}$ chart. On the other hand, inclination of such curves with respect to the equilibrium line is low, so that small changes in the variables (e.g. due to inaccurate average sizes or significant polydispersion, uncertainties of the voidage value and its dependence on composition)

may result in significant influence on the accuracy of the predictions, partly justifying the difficulties in catching the exact critical values.

Also, it should not be forgotten that the initial fluidization process (i.e. the transition from the fixed to the fluidized bed with gas velocity) for a mixture is not an on-off process and it is not infrequent that below or above the suspended part of bed, solids become packed again as a result of the transient and possibly limited segregation process. After such changes in the local bed composition the model predictions can no longer be considered applicable, at least on the global scale. Therefore, the model predictions shall be intended only as initial segregation direction starting from a mixed bed.

In summary, also in consideration of the fact that no relations had previously proposed to predict the tendency toward the correct segregation pattern, the discrimination between the two segregation directions predicted by the PSM appears in good agreement with the available data. Additional verification of the predicted tendency and possibly to its reversal with bed composition is necessary to further assess the validity of the proposed model in more general terms.

7. Conclusions

The segregating behavior of components in a gas-fluidized mixture of solids was studied by means of a generalization of the recently proposed Particle Segregation Model (PSM) and the consideration of the minimum fluidization velocity of the mixture constituents. The focus was on the characterization of the segregation patterns of pairs of a small-denser species (HS) and a big-less-dense species (LB) at incipient fluidization, although the results can be extended to other, more trivial, cases. The PSM involves careful evaluation of the drag and buoyancy forces and is based on balances at the particle scale. Coefficients of the force repartition between differently sized particle species are derived in general terms and force dependence on the size ratio is analyzed for the pure drag force (i.e. excluding pressure gradient) and the net force (including pressure gradient) formulations. On this basis, the first result of this work is that the PSM proves valid more in general than previously reported, as the extension to all flow regimes is possible without model modifications. Coupled to the equal minimum fluidization condition, the segregation direction predictions of the PSM allow defining a map of three possible segregation/fluidization scenarios, observable depending upon the combinations of size ratio, density ratio and mixture composition:

1. HS particles segregating at the bottom and LB particles to the top, with the latter being fluidized, for $s < d^2$ in the viscous flow regime and $s < d$ in the inertial regime;

2. HS particles segregating at the bottom and LB particles to the top, with the former being fluidized below a stagnant bed containing the rest of the mixture, for $s > d^2$ or $s > d$ (for viscous and inertial regime, respectively) and s below the (composition dependent) equilibrium curve prescribed by Eq. (27);

3. HS particles segregating and fluidizing at the top of the bed for s above the equilibrium curve prescribed by Eq. (27).

Comparison of model predictions and experiments is carried out in different ways. The occurrence of the most unexpected behavior predicted by the model, i.e. a partially segregated bed fluidized from below (and stagnant at the top), is demonstrated in a 2D setup and also reproduced in 3D columns. Predictions of the tendency to float or sink of very large spheres immersed in a fluidized bed were validated with experimental data available in the literature. Finally, the capabilities of the PSM to prescribe the segregation tendency or "direction" of binary mixtures were assessed by comparison with an extensive set of measurements including 53 systems available in the literature and 7 systems examined in this work. Of particular relevance is the demonstration of the capability to catch, with a reasonable accuracy, change of segregation behavior for the same mixture with bed composition. Further investigations are required to verify the condition of mixing (at low velocity) suggested by the PSM results for systems characterized by properties in the vicinity of the equilibrium curves.

List of symbols

D	particle diameter, m
$\overline{D}$	Sauter's mean particle diameter, m
d	diameter ratio (D_1/D_2), -
$\bar{d}$	average diameter ratio ($\overline{D}/D_2$), -
F_d	pure drag force, N
g	gravitational acceleration, m/s^2
N	net fluid-particle interaction force, N
$\overline{N}$	spatially averaged net fluid-particle force, N
p	*net* pressure, Pa
$\overline{Re}$	average Reynolds number, -
s	inverse density ratio (ρ_2/ρ_1), -
$\bar{s}$	inverse average density ratio ($\rho_2/\bar{\rho}$), -
u	superficial fluid-to-particle relative velocity, m/s
u_{mf}	minimum fluidization velocity, m/s
$\bar{u}_{mf}$	average minimum fluidization velocity, m/s
V_p	particle volume, m^3
x	fluid-free solids volumetric fraction, -
y	polydispersion index $y_i = D_i/\overline{D}$, -
z	vertical coordinate, m

Greek symbols

α	species-to-average net fluid-particle force ratio, -
β	species-to-average pure drag force ratio, -
ε	voidage, -
μ	fluid viscosity, Pa·s
ρ	solid density, kg/m^3
$\bar{\rho}$	average solid density, kg/m^3
ρ_f	fluid density, kg/m^3

Subscripts

1, 2	index for solid species
Exp	experiments
i, j	relative to the *i*-th, or *j*-th particle or particle species
Sim	simulations

Acronyms

LB	Bigger-less-dense species
PSM	Particle Segregation Model
HS	Smaller-denser species

References

Beeckmans, J.M., Stahl, B., 1987. Mixing and segragation kinetics in a strongly segregated gas-fluidized bed. Powder Technology 53, 31–38.

Beetstra, R., Van der Hoef, M.A., Kuipers, J.A.M., 2007. Numerical study of segregation using a new drag force correlation for polydisperse systems derived from lattice-Boltzmann simulations. Chemical Engineering Science 62, 246–255.

Bokkers, G.A., Van Sint Annaland, M., Kuipers, J.A.M., 2004. Mixing and segregation in a bidisperse gas–solid fluidised bed: a numerical and experimental study. Powder Technology 140, 176–186.

Cello, F., Di Renzo, A., Di Maio, F.P., 2010. A semi-empirical model for the drag force and fluid–particle interaction in polydisperse suspensions. Chemical Engineering Science 65, 3128–3139.

Chao, Z., Wang, Y., Jakobsen, J.P., Fernandino, M., Jakobsen, H.A., 2012. Multi-fluid modeling of density segregation in a dense binary fluidized bed. Particuology 10, 62–71.

Chiba, S., Chiba, T., Nienow, A.W., Kobayashi, H., 1979. The minimum fluidisation velocity, bed expansion and pressure-drop profile of binary particle mixtures. Powder Technology 22, 255–269.

Chiba, S., Nienow, A.W., Chiba, T., Kobayashi, H., 1980. Fluidised binary mixtures in which the denser component may be flotsam. Powder Technology 26, 1–10.

Cui, H., Grace, J.R., 2007. Fluidization of biomass particles: A review of experimental multiphase flow aspects. Chemical Engineering Science 62, 45–55.

Dahl, S.R., Hrenya, C.M., 2005. Size segregation in gas–solid fluidized beds with continuous size distributions. Chemical Engineering Science 60, 6658–6673.

Di Felice, R., 1994. The voidage function for fluid-particle interaction systems. International Journal of Multiphase Flow 20, 153–159.

Di Maio, F.P., Di Renzo, A., Vivacqua, V., 2012. A particle segregation model for gas-fluidization of binary mixtures. Powder Technology 226, 180–188.

Di Renzo, A., Cello, F., Di Maio, F.P., 2011. Simulation of the layer inversion phenomenon in binary liquid--fluidized beds by DEM–CFD with a drag law for polydisperse systems. Chemical Engineering Science 66, 2945–2958.

Di Renzo, A., Di Maio, F.P., Girimonte, R., Formisani, B., 2008. DEM simulation of the mixing equilibrium in fluidized beds of two solids differing in density. Powder Technology 184, 214–223.

Di Renzo, A., Di Maio, F.P., Vivacqua, V., 2012. Prediction of the Flotsam Component in a Gas-Fluidized Bed of Two Dissimilar Solids. International Journal of Chemical Reactor Engineering 10, A26.

Ekinci, E., Atakül, H., Tolay, M., 1990. Detection of segregation tendencies in a fluidised bed using temperature profiles. Powder Technology 61, 185–192.

Ergun, S., 1952. Fluid flow through packed columns. Chemical Engineering Progress 48, 89–94.

Feng, Y.Q., Xu, B.H., Zhang, S.J., Yu, A.B., Zulli, P., 2004. Discrete particle simulation of gas fluidization of particle mixtures. AIChE Journal 50, 1713–1728.

Feng, Y.Q., Yu, A.B., 2007. Microdynamic modelling and analysis of the mixing and segregation of binary mixtures of particles in gas fluidization. Chemical Engineering Science 62, 256–268.

Formisani, B., De Cristofaro, G., Girimonte, R., 2001. A fundamental approach to the phenomenology of fluidization of size segregating binary mixtures of solids. Chemical Engineering Science 56, 109–119.

Formisani, B., Girimonte, R., Longo, T., 2008a. The fluidization process of binary mixtures of solids: Development of the approach based on the fluidization velocity interval. Powder Technology 185, 97–108.

Formisani, B., Girimonte, R., Longo, T., 2008b. The fluidization pattern of density-segregating binary mixtures. Chemical Engineering Research and Design 86, 344–348.

Formisani, B., Girimonte, R., Vivacqua, V., 2011. Fluidization of mixtures of two solids differing in density or size. AIChE Journal 57, 2325–2333.

Formisani, B., Girimonte, R., Vivacqua, V., 2012. Fluidization of mixtures of two solids: A unified model of the transition to the fluidized state. AIChE Journal n/a–n/a.

Gera, D., Syamlal, M., O'Brien, T.J., 2004. Hydrodynamics of particle segregation in fluidized beds. International Journal of Multiphase Flow 30, 419–428.

Gibilaro, L.G., Di Felice, R., Waldram, S.P., Foscolo, P.U., 1986. A predictive model for the equilibrium composition and inversion of binary-solid liquid fluidized beds. Chemical Engineering Science 41, 379–387.

Gibilaro, L.G., Rowe, P.N., 1974. A model for a segregating gas fluidised bed. Chemical Engineering Science 29, 1403–1412.

Gilbertson, M.A., Eames, I., 2001. Segregation patterns in gas-fluidized systems 433, 347–356.

Hoffmann, A.C., Janssen, L.P.B.M., Prins, J., 1993. Particle segregation in fluidised binary mixtures. Chemical Engineering Science 48, 1583–1592.

Holloway, W., Yin, X., Sundaresan, S., 2009. Fluid-particle drag in inertial polydisperse gas-solid suspensions. AIChE Journal 56, 1995–2004.

Hoomans, B.P.B., Kuipers, J.A.M., Van Swaaij, W.P.M., 2000. Granular dynamics simulation of segregation phenomena in bubbling gas-fluidised beds. Powder Technology 109, 41–48.

Huilin, L., Yurong, H., Gidaspow, D., 2003. Hydrodynamic modelling of binary mixture in a gas bubbling fluidized bed using the kinetic theory of granular flow. Chemical Engineering Science 58, 1197–1205.

Jang, H.T., Park, T.S., Cha, W.S., 2010. Mixing–segregation phenomena of binary system in a fluidized bed. Journal of Industrial and Engineering Chemistry 16, 390–394.

Joseph, G.G., Leboreiro, J., Hrenya, C.M., Stevens, A.R., 2007. Experimental segregation profiles in bubbling gas-fluidized beds. AIChE Journal 53, 2804–2813.

Kunii, D., Levenspiel, O., 1991. Fluidization Engineering. Butterworth-Heinemann, Boston.

Marzocchella, A., Salatino, P., Di Pastena, V., Lirer, L., 2000. Transient fluidization and segregation of binary mixtures of particles. AIChE Journal 46, 2175–2182.

Mazzei, L., Casillo, A., Lettieri, P., Salatino, P., 2010. CFD simulations of segregating fluidized bidisperse mixtures of particles differing in size. Chemical Engineering Journal 156, 432–445.

Naimer, N.S., Chiba, T., Nienow, A.W., 1982. Parameter estimation for a solids mixing|segregation model for gas fluidised beds. Chemical Engineering Science 37, 1047–1057.

Nienow, A.W., Rowe, P.N., Cheung, L.Y.-L., 1978. A quantitative analysis of the mixing of two segregating powders of different density in a gas-fluidised bed. Powder Technology 20, 89–97.

Okayama, Y., Doi, A., Kawaguchi, T., Tanaka, T., Tsuji, Y., 2006. Drag Force Model for Fluidized Bed of Binary Mixture of Particles, in: Proceedings of the 5th World Congress on Particle Technology.

Olivieri, G., Marzocchella, A., Salatino, P., 2004. Segregation of fluidized binary mixtures of granular solids. AIChE Journal 50, 3095–3106.

Olivieri, G., Marzocchella, A., Salatino, P., 2009. A fluid-bed continuous classifier of polydisperse granular solids. Journal of the Taiwan Institute of Chemical Engineers 40, 638–644.

Oshitani, J., Ono, K., Ijiri, M., Tanaka, Z., 2004. Effect of particle fluidization intensity on floating and sinking of objects in a gas–solid fluidized bed. Advanced Powder Technology 15, 201–213.

Owoyemi, O., Mazzei, L., Lettieri, P., 2007. CFD modeling of binary-fluidized suspensions and investigation of role of particle-particle drag on mixing and segregation. AIChE Journal 53, 1924–1940.

Qiaoqun, S., Huilin, L., Wentie, L., Yurong, H., Lidan, Y., Gidaspow, D., 2005. Simulation and experiment of segregating/mixing of rice husk–sand mixture in a bubbling fluidized bed. Fuel 84, 1739–1748.

Rao, A., Curtis, J.S., Hancock, B.C., Wassgren, C., 2011. Classifying the fluidization and segregation behavior of binary mixtures using particle size and density ratios. AIChE Journal 57, 1446–1458.

Rasul, M.G., Rudolph, V., 2000. Fluidized bed combustion of Australian bagasse. Fuel 79, 123–130.

Rasul, M.G., Rudolph, V., Čársky, M., 1999. Segregation potential in binary gas fluidized beds. Powder Technology 103, 175–181.

Rowe, P.N., Nienow, A.W., 1976. Particle Mixing and Segregation in Gas Fluidised Beds. A Review. Powder Technology 15, 141–147.

Rowe, P.N., Nienow, A.W., Agbim, A.J., 1972. The Mechanisms by which Particles Segregate in Gas Fluidised Beds - Binary Systems of Near-Spherical particles. Transactions of the Institution of Chemical Engineers 50, 310–323.

Sarkar, S., Van der Hoef, M.A., Kuipers, J.A.M., 2009. Fluid–particle interaction from lattice Boltzmann simulations for flow through polydisperse random arrays of spheres. Chemical Engineering Science 64, 2683–2691.

Tanaka, Z., Song, X., 1996. Continuous separation of particles by fluidized beds. Advanced Powder Technology 7, 29–40.

Van der Hoef, M.A., Beetstra, R., Kuipers, J.A.M., 2005. Lattice-Boltzmann simulations of low-Reynolds-number flow past mono- and bidisperse arrays of spheres: results for the permeability and drag force. Journal of Fluid Mechanics 528, 233–254.

Wu, S.Y., Baeyens, J., 1998. Segregation by size difference in gas fluidized beds. Powder Technology 98, 139–150.

Yin, X., Sundaresan, S., 2009. Fluid-particle drag in low-Reynolds-number polydisperse gas-solid suspensions. AIChE Journal 55, 1352–1368.

Zhou, Z.Y., Yu, A.B., 2009. Simulation of the Flow and Segregation of Particle Mixtures in Liquid Fluidization, in: Powders and Grains. AIP Conference Proceedings 1145, pp. 1–4.

Čársky, M., Pata, J., Veselý, V., Hartman, M., 1987. Binary system fluidized bed equilibrium. Powder Technology 51, 237–242.

Figure Captions

Figure 1. Sketch of the evolution towards possible fluidization and segregation scenarios for initially mixed LB-HS binary beds.

Figure 2. Dependence of the pure drag force ratio (a) and net drag force ratio (b) on the size ratio. The pure drag force ratio plot is unique, while the net drag force ratio depends moderately on composition and voidage (values in the legend).

Figure 3. Segregation direction map with equilibrium lines at voidage $\varepsilon = 0.4$. Part (a) shows the map in terms of species property ratios (Eq. 27) at different compositions; in part (b) the equilibrium line is plotted in terms of the average properties and those of species 2 (Eq. 24). In the sketches, arrows next to each particle type represent the segregation direction.

Figure 4. Segregation direction equilibria and equal minimum fluidization velocity curves for viscous (a) and inertial flows (b). Segregation/fluidization combinations give rise to behaviors as diagrammatically shown by sketches A, B and C and the corresponding zones in the map.

Figure 5. Sequence of photographs showing three different time instants during the fluidization of a mixture of 570 μm diameter glass ballotini (ρ = 2480 kg/m^3) and 229 μm diameter steel shots (ρ = 7600 kg/m^3). The lower, bubbling layer is nearly pure in steel shots and the upper, static layer is a glass-rich mixture.

Figure 6. Comparison of model predictions and experimental observations for the segregation direction in the examined systems (see Table 5). Each experimental datum is shown with a symbol corresponding to the flotsam component (small solid symbols for the HS species and big open symbols for the LB species) in segregated systems or crosses for systems reported as mixed. Model predictions are discriminated by the curve, as shown in Fig. 3b, i.e. the HS (LB) species acts as flotsam above (below) the curve.

Figure 7. Analysis of the systems exhibiting a change of segregation direction in experiments and comparison with the predicted change upon crossing the theoretical equilibrium line. Data from Naimer et al. (1982) and Joseph et al. (2007) (a), Formisani et al. (2008a) (b), Chiba et al. (1980) (c) and this work (d).

Figure01.eps
Click here to download Figure: Figure01.eps

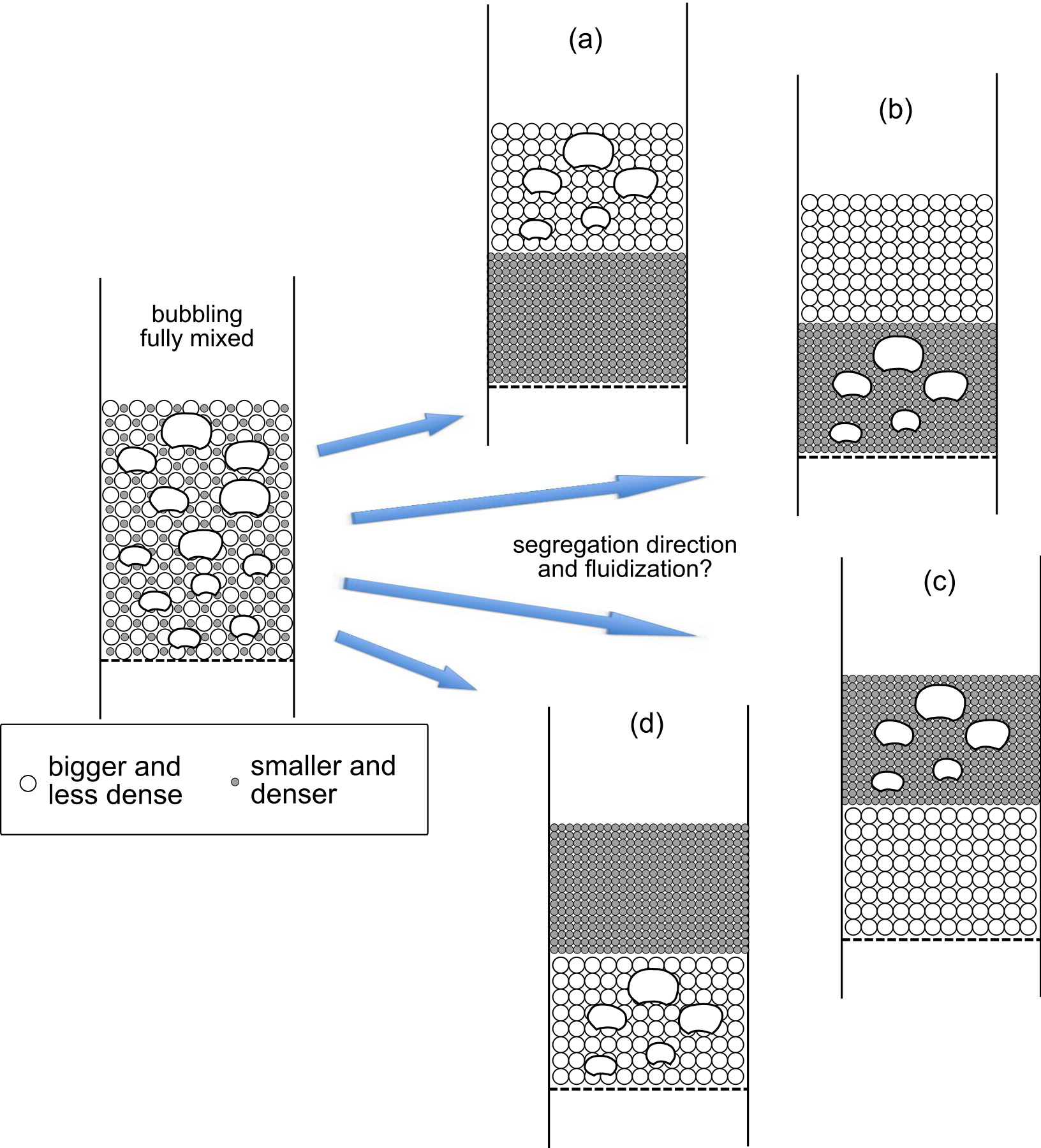

Figure02a.eps
Click here to download Figure: Figure02a.eps

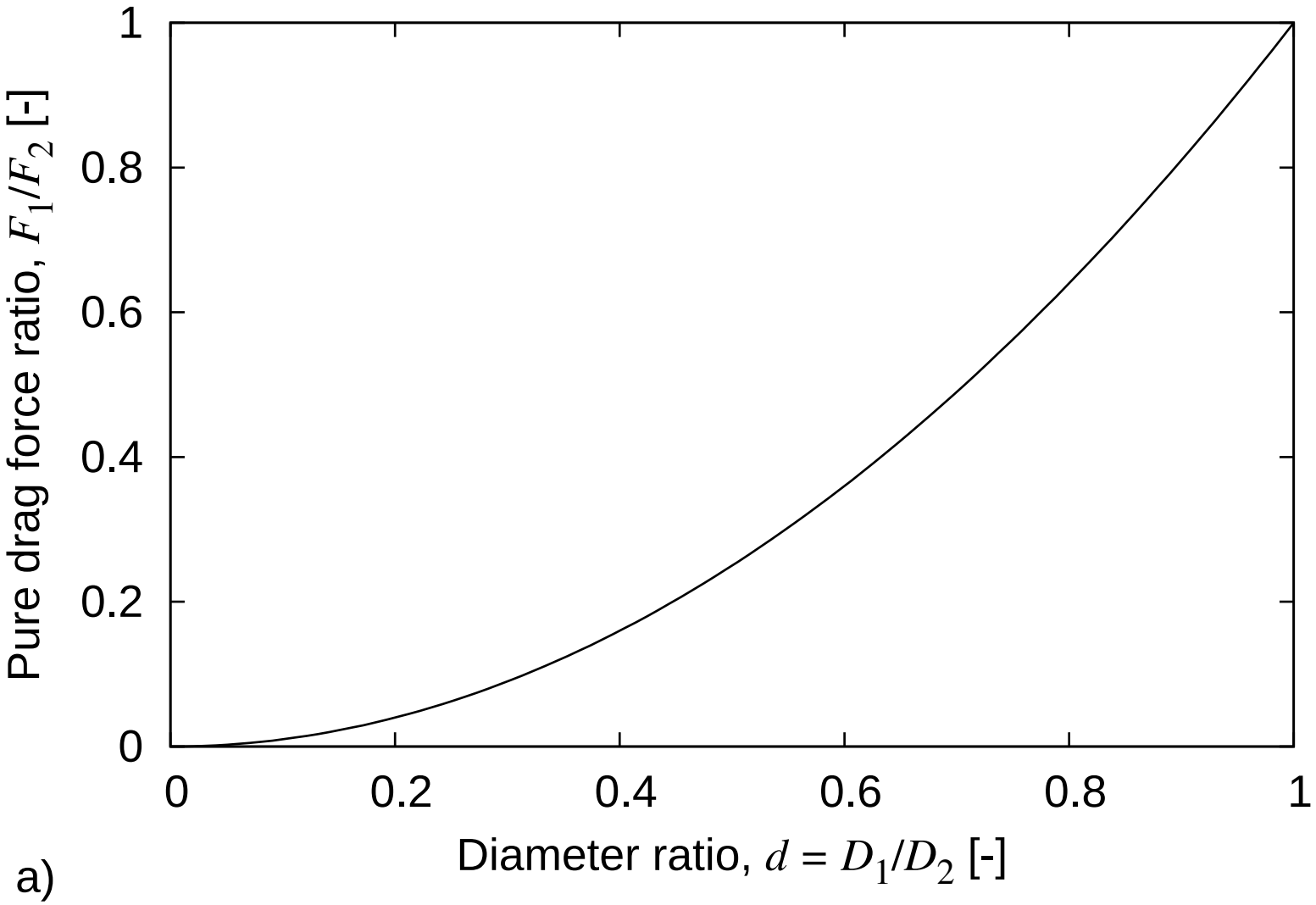

a)

Figure02b.eps
Click here to download Figure: Figure02b.eps

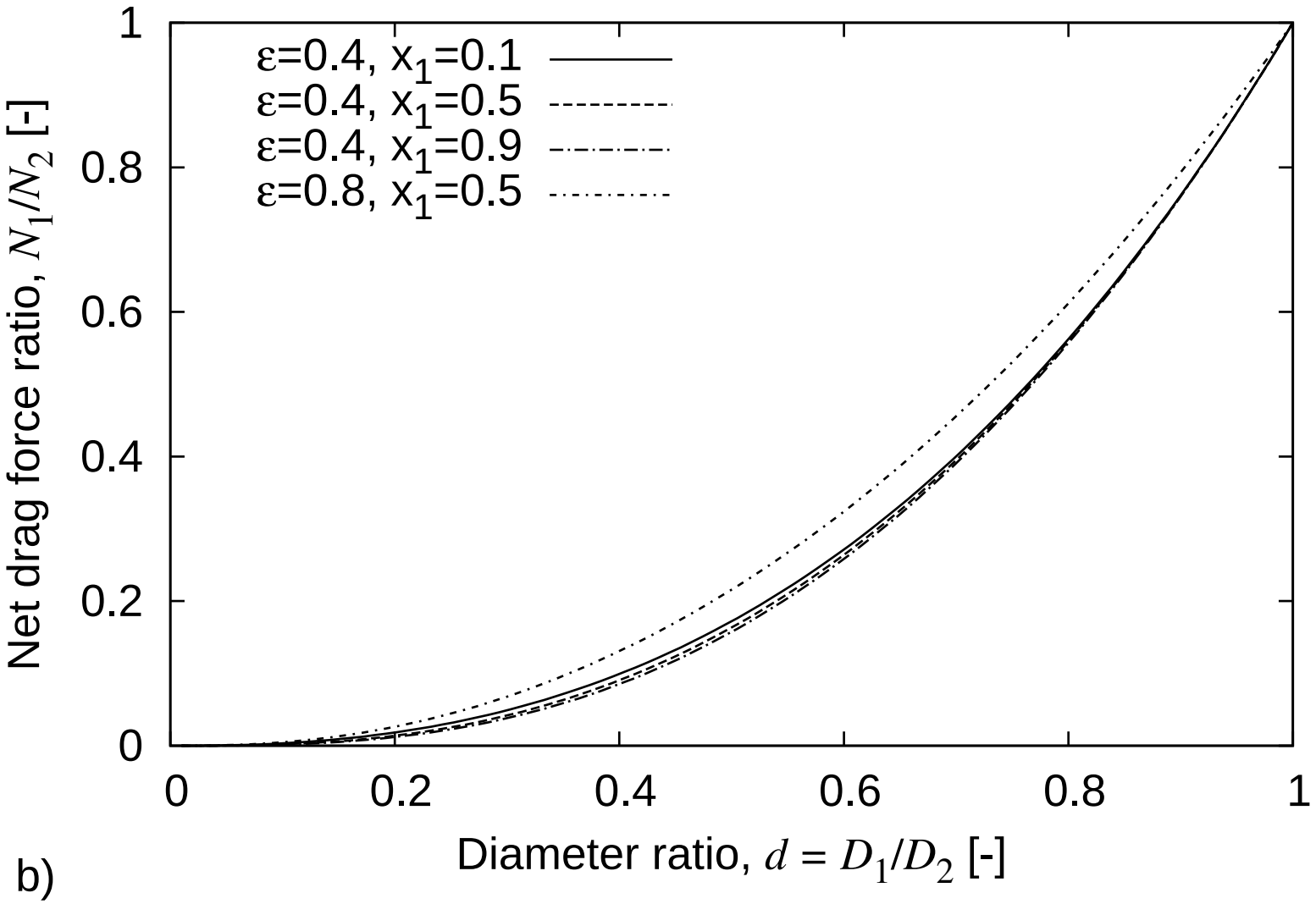

b)

Figure03a.eps
Click here to download Figure: Figure03a.eps

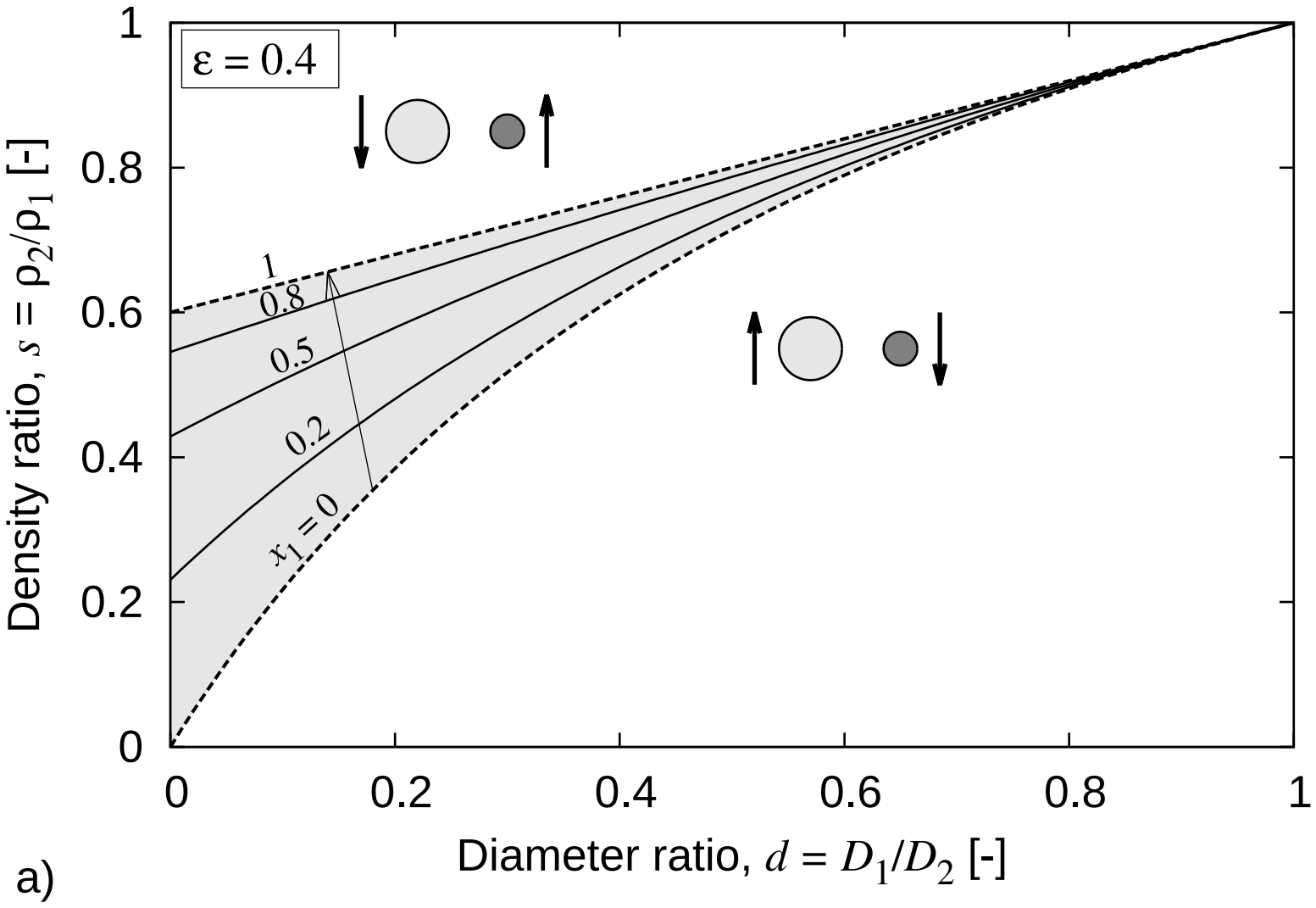

a)

Figure03b.eps
Click here to download Figure: Figure03b.eps

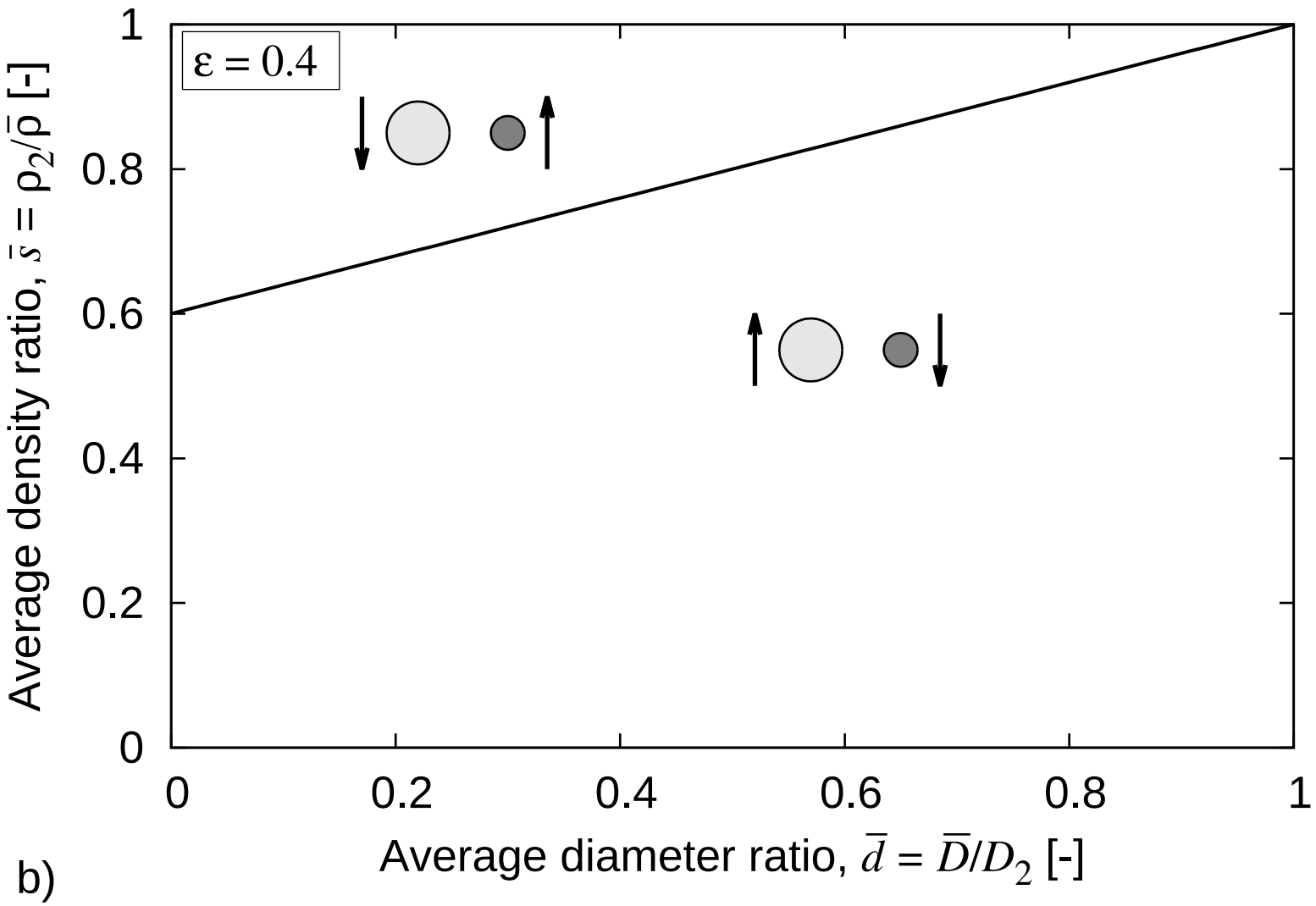

b)

Figure04a.eps
Click here to download Figure: Figure04a.eps

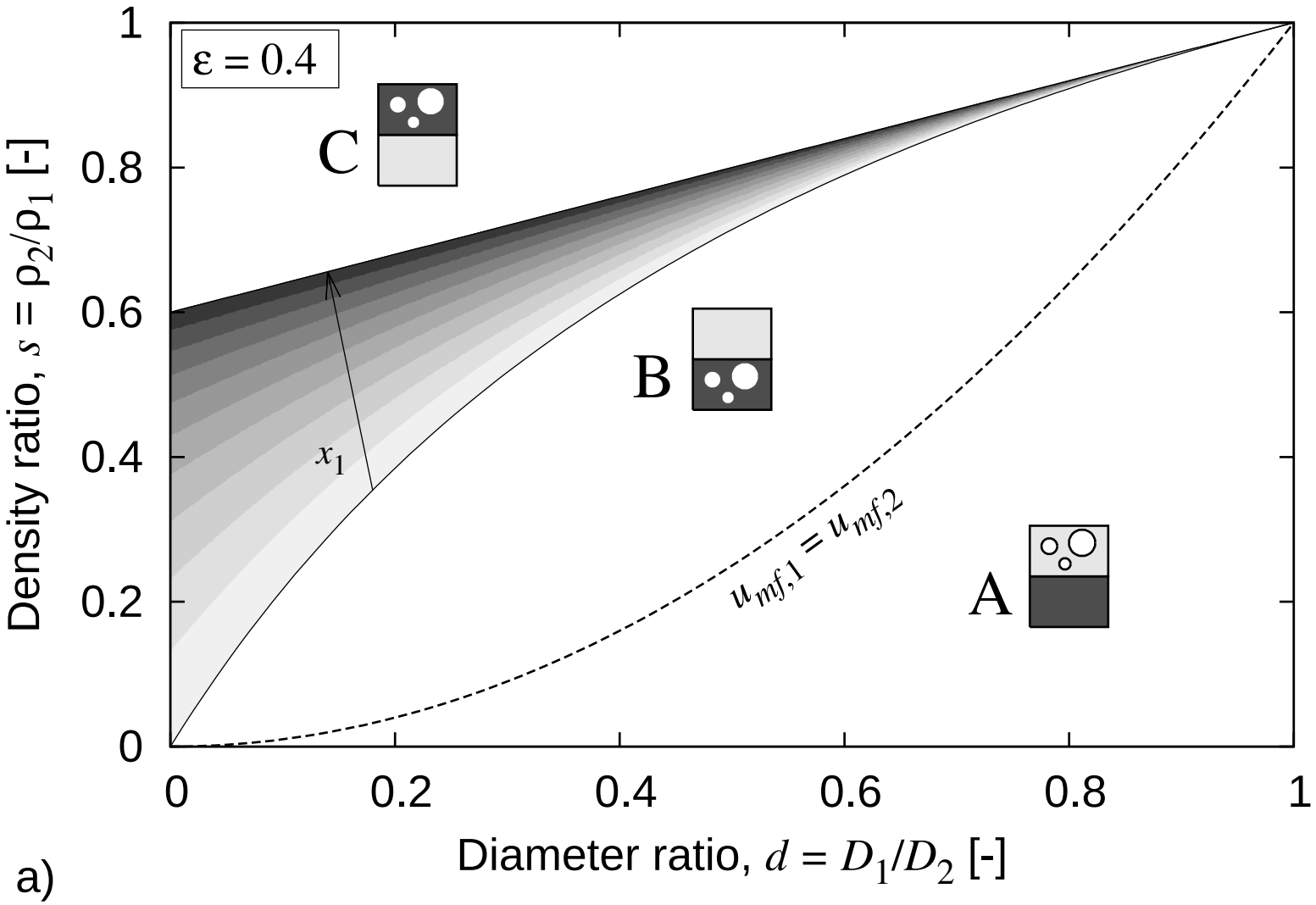

a)

Figure04b.eps
Click here to download Figure: Figure04b.eps

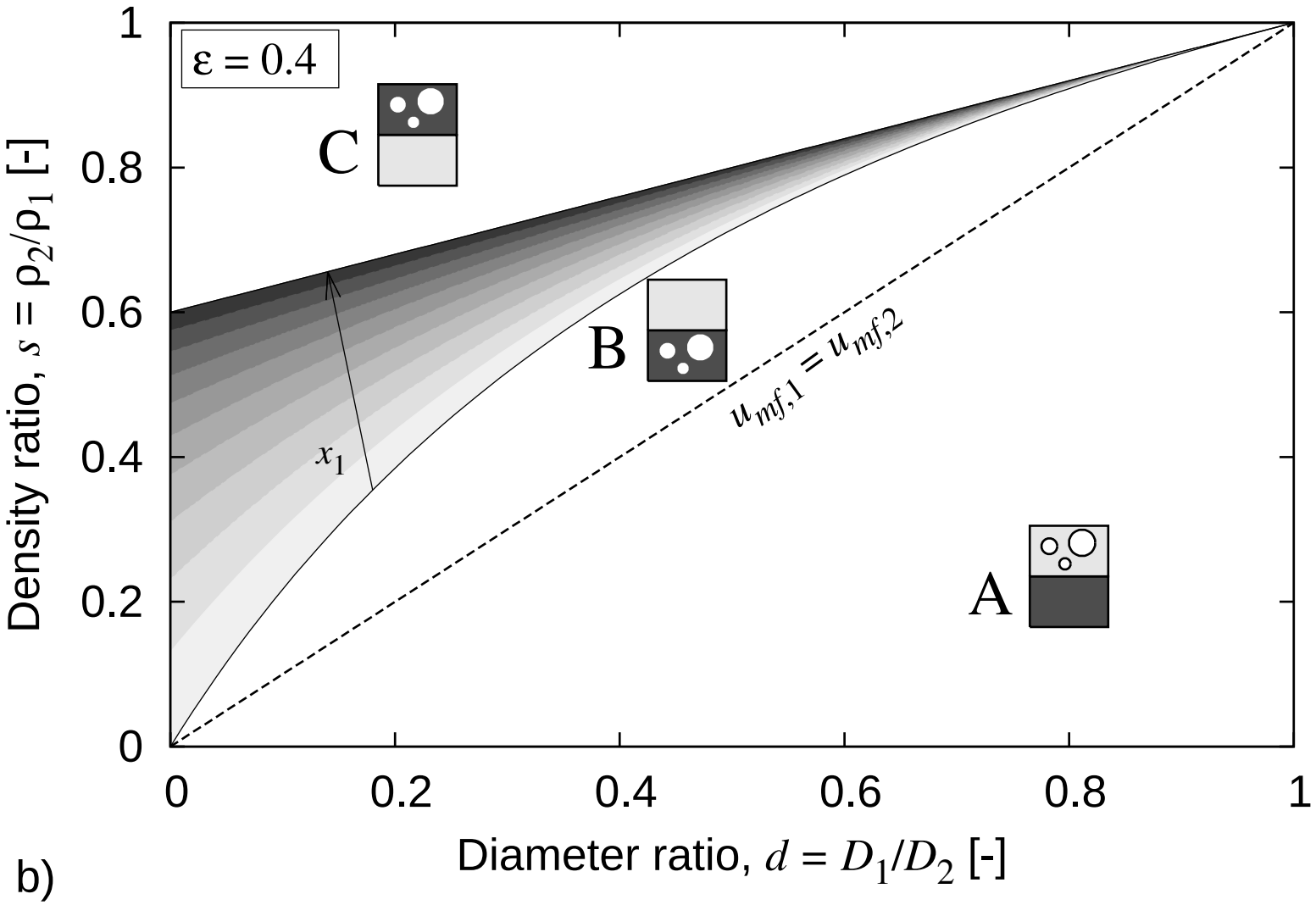

b)

Figure05a.tif
Click here to download high resolution image

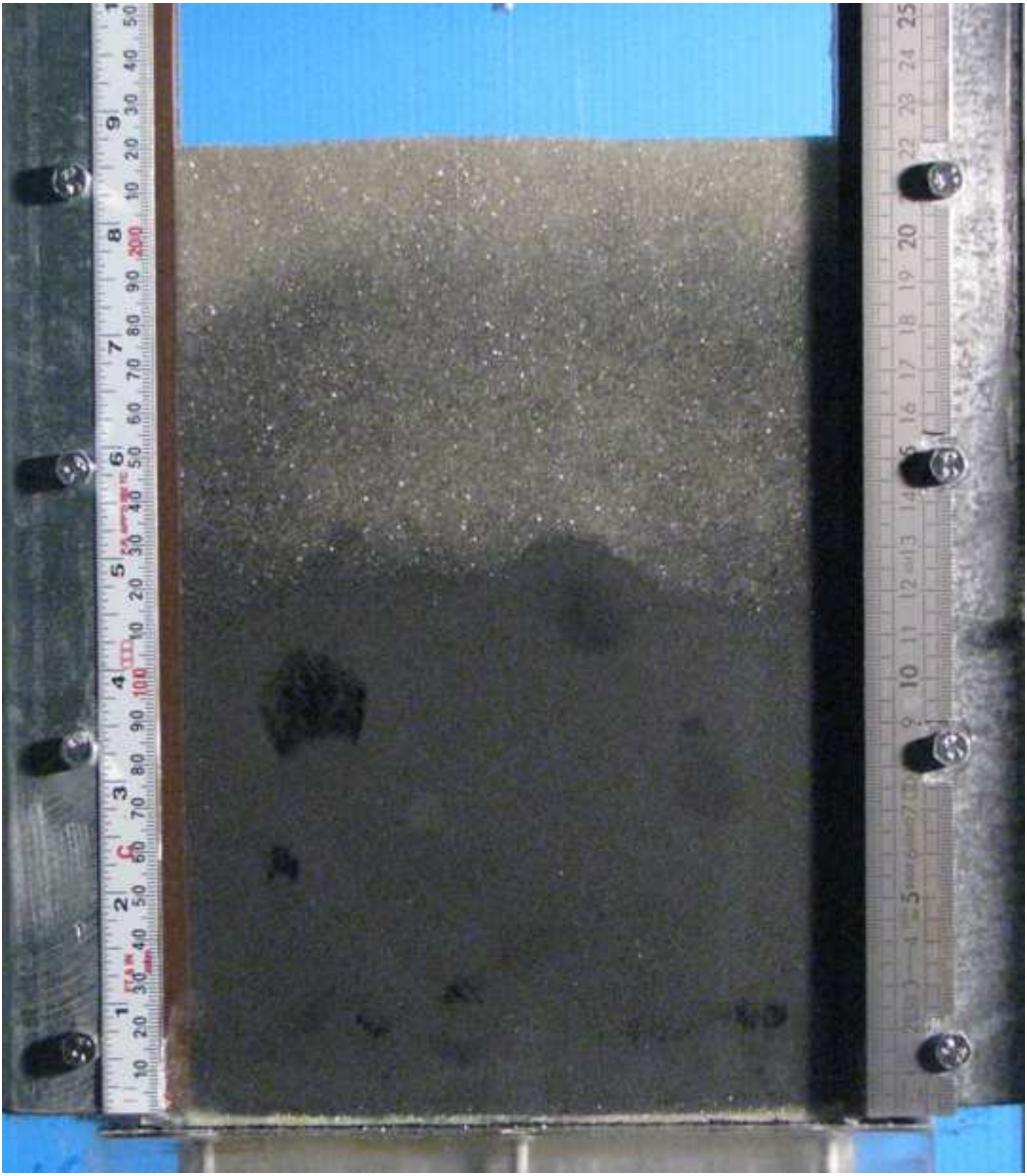

Figure05b.tif
Click here to download high resolution image

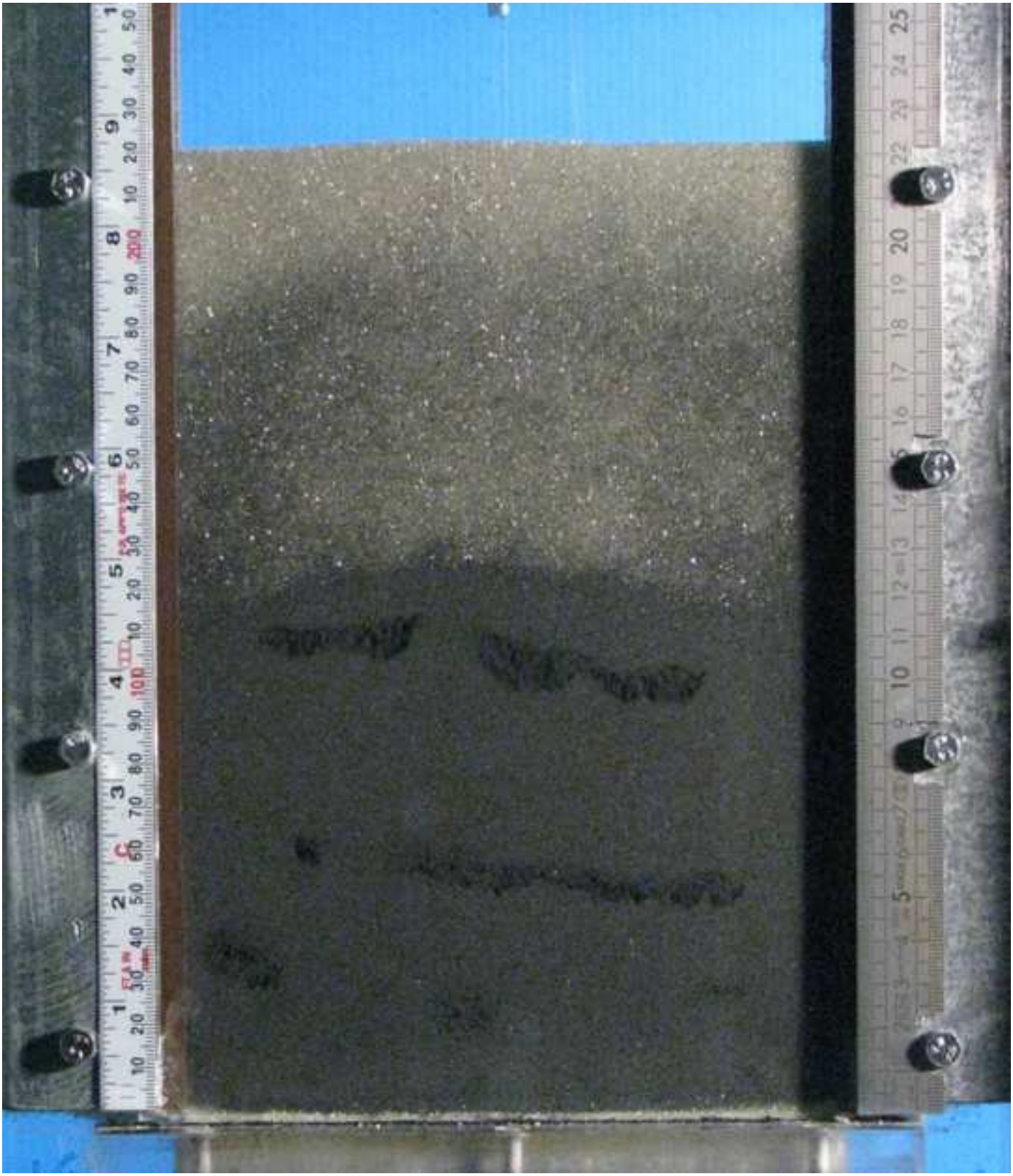

Figure05c.tif
Click here to download high resolution image

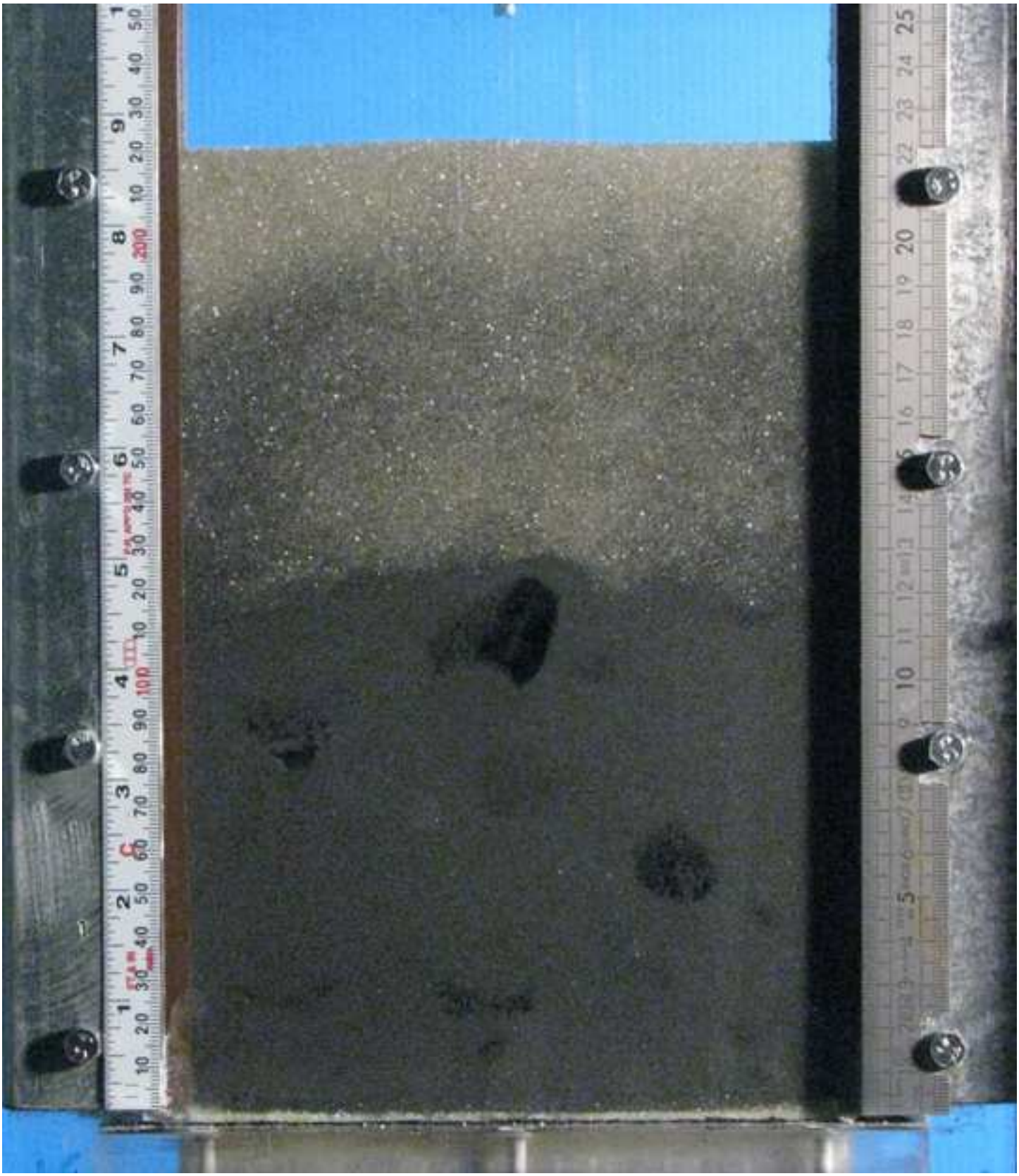

Figure06.eps
Click here to download Figure: Figure06.eps

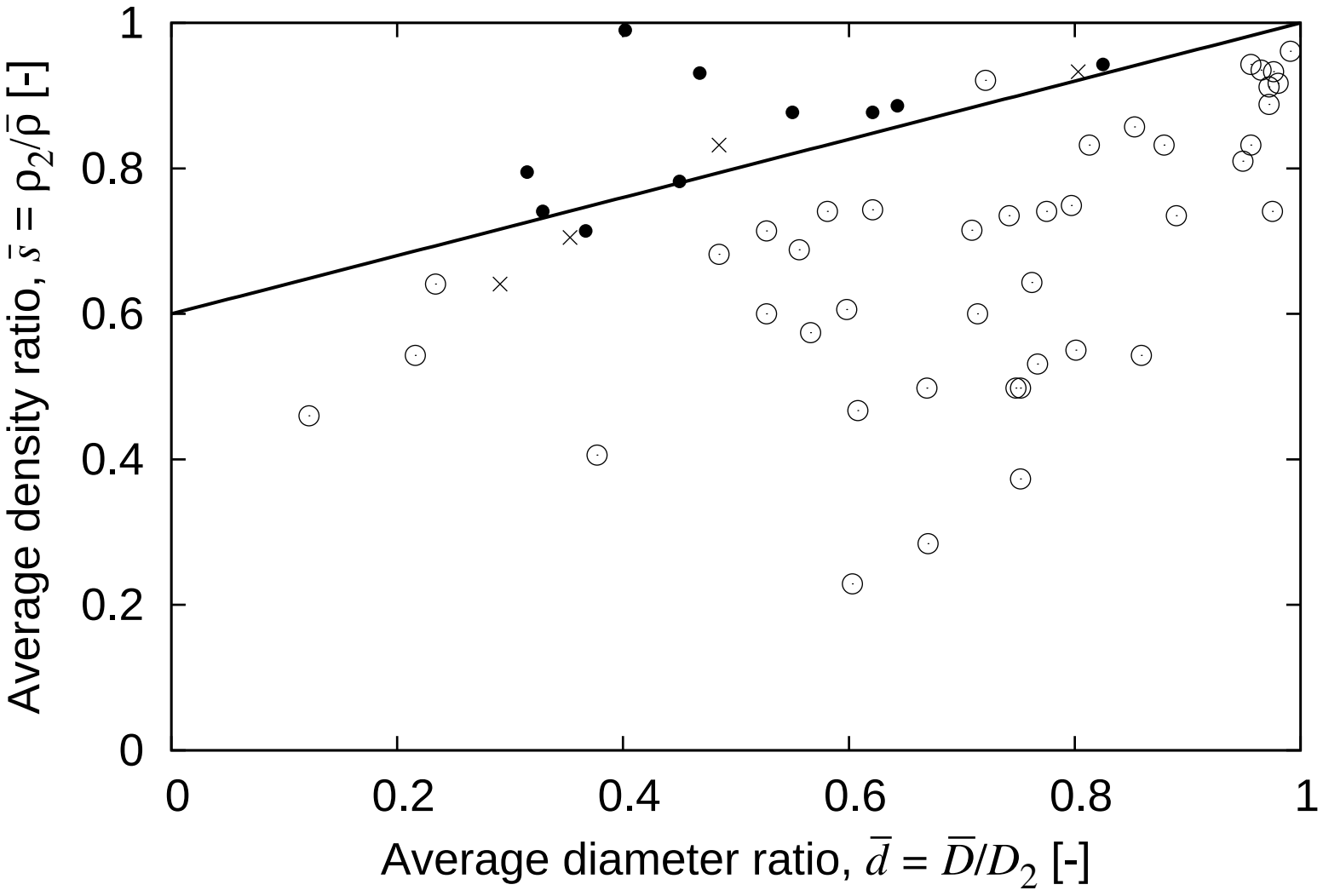

Figure07a.eps
Click here to download Figure: Figure07a.eps

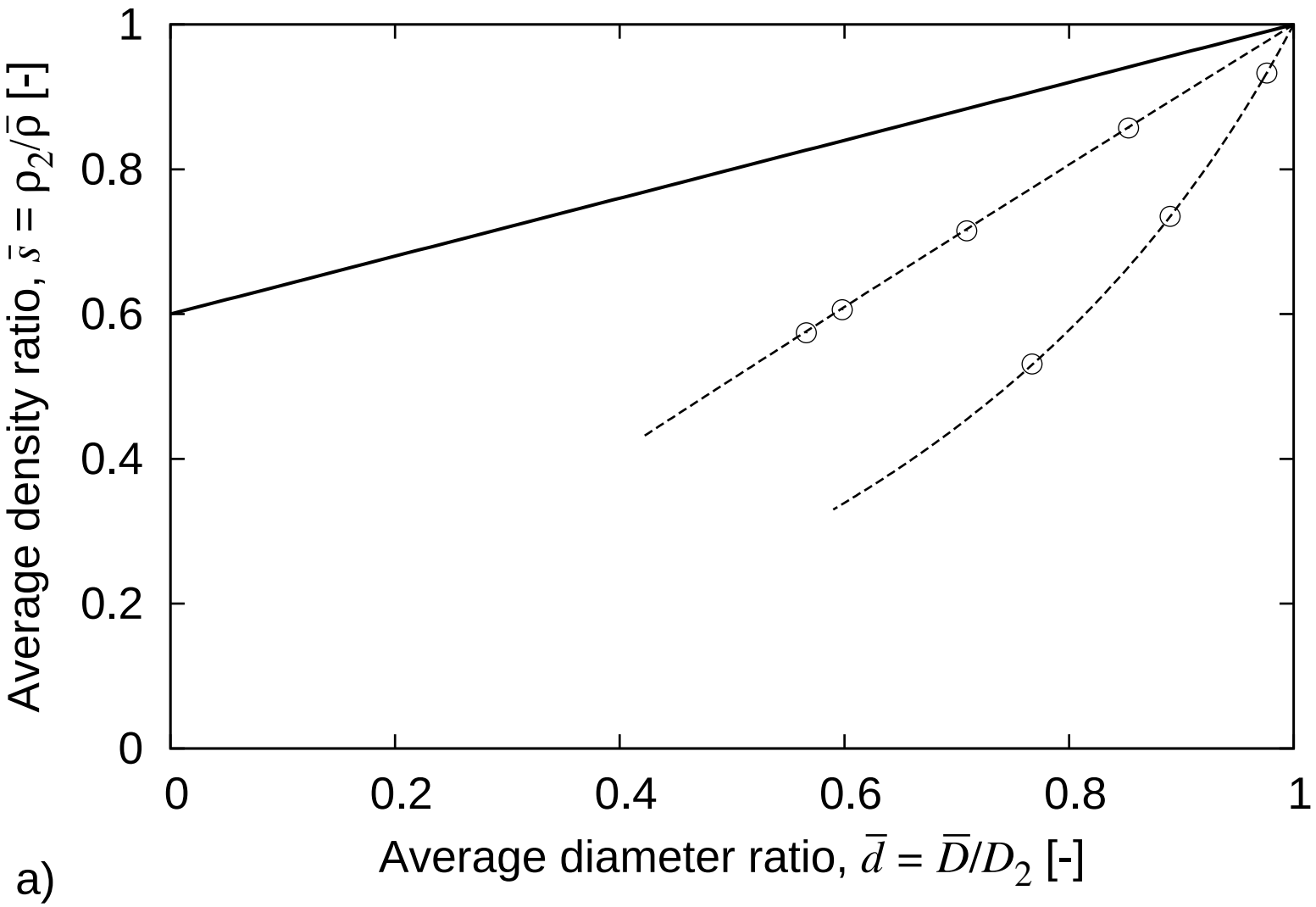

a)

Figure07b.eps
Click here to download Figure: Figure07b.eps

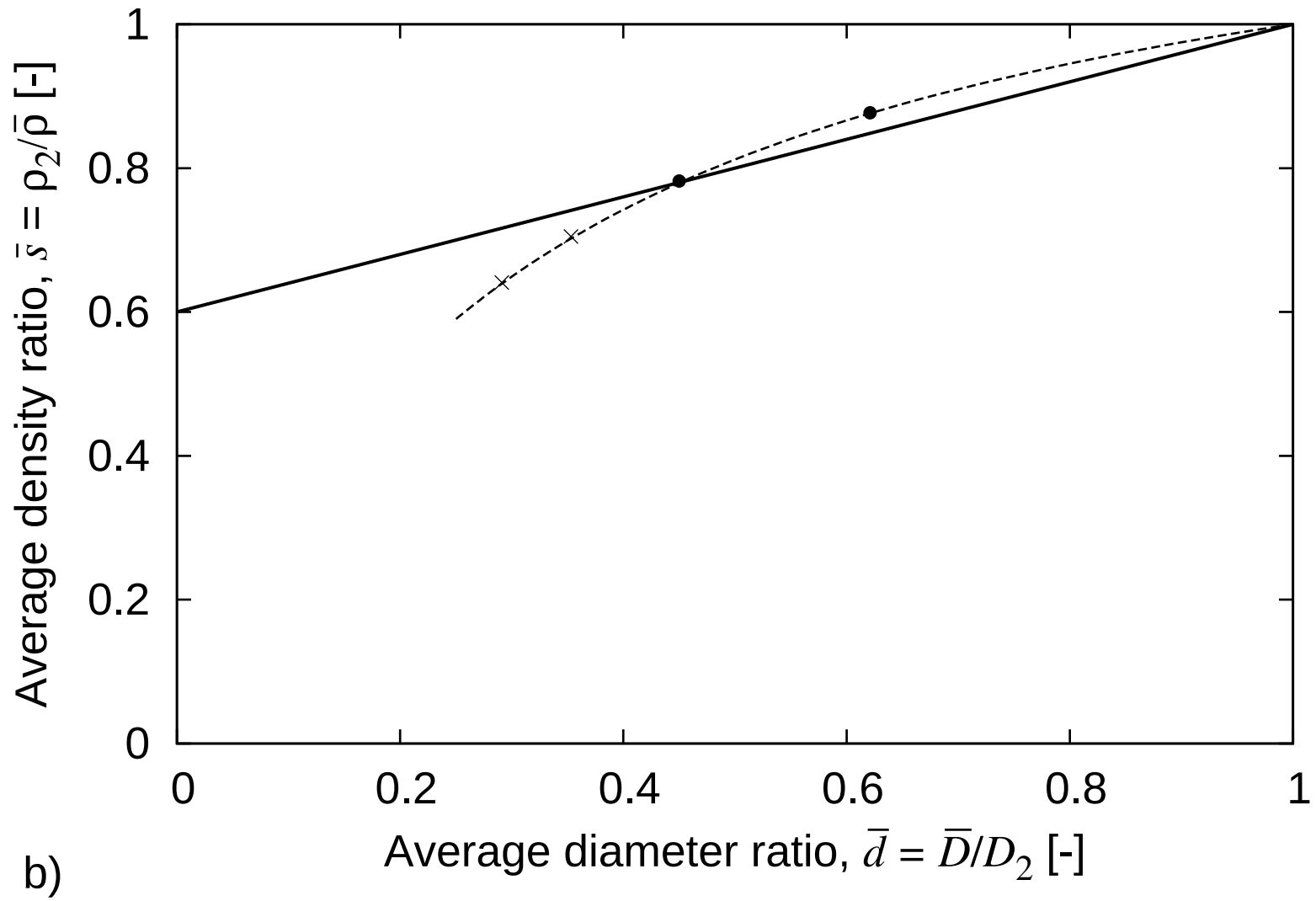

b)

Figure07c.eps
Click here to download Figure: Figure07c.eps

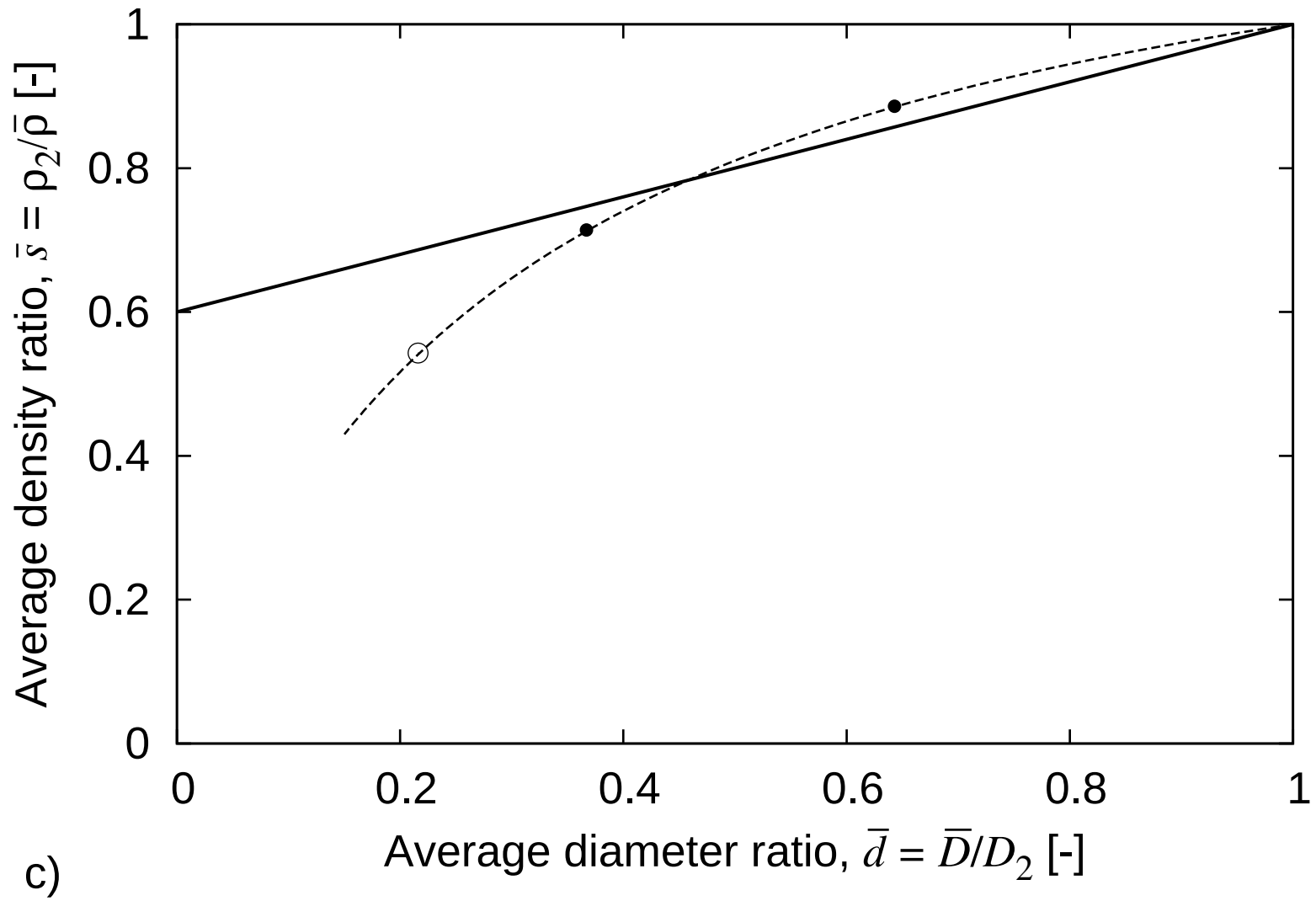

c)

Figure07d.eps
Click here to download Figure: Figure07d.eps

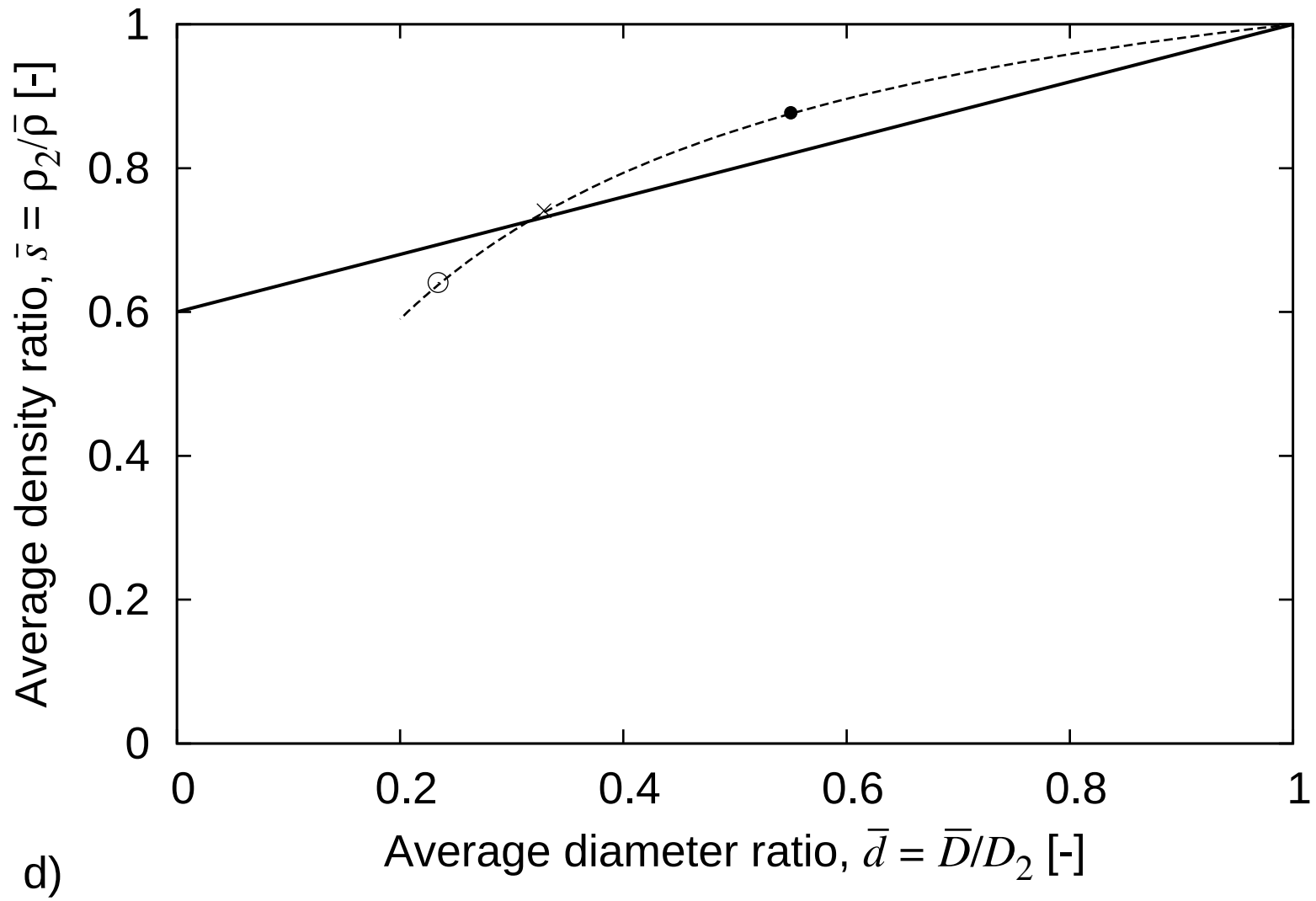

d)

Table 1. Examples of expressions for the specification coefficients compatible with the constraints (Eqs 6, 10 and 13).

Case	a	b	α_k	β_k
1	ε	1	$\varepsilon y_k^2 + (1-\varepsilon) y_k^3$	y_k^2
2	1	$\frac{1}{\varepsilon}$	y_k^2	$\frac{1}{\varepsilon} y_k^2 - \frac{(1-\varepsilon)}{\varepsilon} y_k^3$
3	0	0	y_k^3	y_k^3

Table 2. Properties of the solids.

Solid	Sieve range [μm]	D [μm]	ρ [kg /m^3]
Glass beads (GB)	150-200	162	2480
	300-350	337	
	500-600	521	
	800-1000	898	
Molecular Sieves (MS)	800-900	824	1460
Steel shots (SS)	200-225	229	7600
Bronze shots (BS)	50-100	70	8720
Zirconium silicate spheres (ZS)	150-200	168	3760

Table 3. Properties of the binary mixtures.

No.	Mixture (HS-LB)	d [-]	s [-]	x_1 [-]	$\bar{d}$ [-]	$\bar{s}$ [-]
1	GB521-MS824	0.63	0.59	0.5	0.77	0.74
2	GB337-MS824	0.41	0.59	0.5	0.58	0.74
3	GB162-MS824	0.20	0.59	0.2	0.55	0.88
4	GB162-MS824	0.20	0.59	0.5	0.33	0.74
5	GB162-MS824	0.20	0.59	0.8	0.23	0.64
6	BS70-SS229	0.31	0.87	0.5	0.47	0.93
7	ZS168-GB898	0.19	0.66	0.5	0.32	0.79

Table 4. Flotsam/jetsam behaviour of large particles, species 2, immersed in a fluidized bed of a different solid, species 1. From Oshitani et al. (2004) Model predictions are practically independent of the volumetric fraction of the immersed spheres and the reported values are for the limit $x_1 = 1$.

No.	Solids (1 / 2)	D_1 [μm]	ρ_1 [kg/m^3]	D_2 [μm]	ρ_2 [kg/m^3]	d	s	*Exp. flotsam*	*Model flotsam*
1	Glass / 6-Nylon	275	2500	2370	1120	0.12	0.45	2	2
2	Glass / 6-Nylon	275	2500	4760	1120	0.06	0.45	2	2
3	Glass / 6-Nylon	275	2500	7940	1120	0.03	0.45	2	2
4	Glass / 6-Nylon	275	2500	11110	1120	0.02	0.45	2	2
5	Glass / 6-Nylon	275	2500	19050	1120	0.01	0.45	2	2
6	Glass / Teflon	655	2500	4760	1680	0.14	0.67	1	1
7	Glass / Teflon	463	2500	4760	1680	0.10	0.67	1	1
8	Glass / Teflon	275	2500	4760	1680	0.06	0.67	1	1

Table 5. Properties of the systems considered for model validation.

Reference	D_1 [μm]	ρ_1 [kg/m^3]	D_2 [μm]	ρ_2 [kg/m^3]	d	s	x_1*	flotsam exper.	flotsam model
(Rowe et al., 1972)	82	8860	271	2940	0.30	0.33	0.10	2	2
---	114	8860	271	2940	0.42	0.33	0.10	2	2
---	114	8860	189	2940	0.60	0.33	n/a	2	2 (any x_1)
---	82	8860	267	1050	0.31	0.12	0.01	2	2
							0.11	2	2
---	82	8860	163	2940	0.50	0.33	n/a	2	2 (any x_1)
(Rowe et al., 1976)	273	8860	461	2950	0.59	0.33	0.04	2	2
							0.18	2	2
							0.44	2	2
---	231	8540	461	2950	0.50	0.35	0.04	2	2
(Chiba et al., 1979)	385	2520	775	1080	0.50	0.43	0.25	2	2
(Chiba et al., 1980)	115	2520	775	1080	0.15	0.43	0.10	1	1
							0.30	1	2
							0.63	2	2
---	194	2520	650	1080	0.30	0.43	0.26	2	2
							0.34	2	2
---	115	2520	650	1080	0.18	0.43	0.05	1	1
---	194	2520	775	1080	0.25	0.43	0.30	2	2
---	385	2520	775	1080	0.50	0.43	0.05	2	2
(Beeckmans and Stahl, 1987)	340	7860	480	2800	0.71	0.36	0.02	2	2
							0.05	2	2
							0.07	2	2
							0.11	2	2
							0.13	2	2
(Čársky et al., 1987)	170	6239	475	2673	0.36	0.43	n/a	2	2 (any x_1)
(Hoffmann et al., 1993)	235	8750	565	2510	0.42	0.29	0.22	2	2
							0.46	2	2
(Rasul et al., 1999)	64	1420	200	492	0.32	0.35	0.78	2	2
---	200	492	2000	200	0.10	0.41	0.80	2	2
---	64	950	200	492	0.32	0.52	n/a	2	2 (any x_1)
---	64	690	200	492	0.32	0.71	n/a	mix	mix (x_1=0.85)
(Rasul and Rudolph, 2000)	64	1420	98	1270	0.65	0.89	0.73	2	1
(Marzocchella et al., 2000)	125	2530	500	2480	0.25	0.98	0.50	1	1
(Olivieri et al., 2004)	125	2600	375	600	0.33	0.23	0.20	2	2
(Joseph et al., 2007)	116	2476	275	1064	0.42	0.43	0.13	2	2
							0.30	2	2
							0.49	2	2
							0.56	2	2
(Formisani et al., 2008a)	154	2480	624	1460	0.25	0.59	0.10	1	1
							0.20	1	1
							0.40	1	1
							0.60	mix	2
							0.80	mix	2
---	439	7600	800	1460	0.55	0.19	0.20	2	2
							0.40	2	2
							0.60	2	2
							0.80	2	2
---	593	2480	624	1460	0.95	0.59	0.50	2	2
(Jang et al., 2010)	715	2620	1545	1190	0.46	0.45	0.30	2	2
(Naimer et al., 1982)	273	8860	461	2950	0.59	0.33	0.04	2	2
							0.18	2	2
							0.44	2	2
---	70	8860	550	2950	0.13	0.33	0.04	mix	mix
This work	521	2480	824	1460	0,63	0,59	0,50	2	2
---	337	2480	824	1460	0,41	0,59	0,50	2	2
---	162	2480	824	1460	0,20	0,59	0,20	1	1
							0,50	mix	1
							0,80	2	2
---	70	8720	229	7600	0,31	0,87	0,50	1	1
---	168	3760	898	2480	0,19	0,66	0,50	1	1

* n/a=not available.